

52-45  
53450

#42

---

# CHAPTER 7

---

N92-15459

## Theory and Observations Model Simulations of the Period 1955 – 1985

### Panel Members

- I. S. A. Isaksen, Chair  $\Phi 2736708$
- R. Eckman
- A. Lacis
- M. Ko — A6525710
- M. Prather — NC999967
- J. Pyle — CE261061
- H. Rodhe
- F. Stordal —  $\Phi 2736708$
- R. Stolarski — NC999967
- R. P. Turco —
- D. Wuebbles — LH075075



## Chapter 7

### Theory and Observations Model Simulations of the Period 1955–1985

#### Contents

7.0	INTRODUCTION .....	503
7.1	ATMOSPHERIC SCENARIOS FOR 1955–1990 .....	503
7.1.1	Trace Gases .....	504
7.1.2	Solar Variability .....	506
7.1.3	Nuclear Test Series .....	507
7.1.4	Atmospheric Variations Not Modelled .....	508
7.2	THE MODELS .....	508
7.2.1	Model Descriptions .....	508
7.2.2	Basic Chemical Uncertainties .....	511
7.2.3	Uncertainties in Transport .....	512
7.2.4	Comparison of Models With the Contemporary Atmosphere .....	513
7.2.5	Stratospheric Temperature Feedbacks .....	521
7.3	MODEL SIMULATIONS OF OZONE CHANGE .....	521
7.3.1	Calculated Total Global Variations .....	522
7.3.2	Atmospheric Nuclear Tests .....	523
7.3.3	Column Ozone: Comparison With Observations .....	525
7.3.3.1	Theoretical Fingerprints for the Solar Cycle and Trace Gases .....	525
7.3.3.2	Thirty Years of Dobson Data .....	527
7.3.3.3	Global Data From Satellite, 1979–1987 .....	527
7.3.3.4	Subtracting the Solar Cycle From Dobson Data .....	531
7.3.4	Profile Ozone: Comparison With Observations .....	532
7.3.4.1	Fingerprints of the Solar Cycle and Trace Gases .....	532
7.3.4.2	Trends in Vertical Structure, 1979–1985 .....	535
7.3.5	Tropospheric Ozone .....	536
7.3.5.1	Impact on Column Perturbations .....	536
7.3.5.2	Uncertainties in the Estimates .....	537
7.3.6	Future Ozone Changes (1985–1990) .....	538
7.3.7	How Good Are the Models? .....	539
7.4	CONCLUSIONS .....	539



## 7.0 INTRODUCTION

The main objective of the theoretical studies presented here is to apply models of stratospheric chemistry and transport in order to understand the processes that control stratospheric ozone and that are responsible for the observed variations. The model calculations are intended to simulate the observed behavior of atmospheric ozone over the past three decades (1955–1985), for which there exists a substantial record of both ground-based and (more recently) satellite measurements. Through comparisons of the modeled history of atmospheric ozone with these data, we hope to:

- Simulate the observed temporal and spatial variations of ozone.
- Focus on the specific patterns, or “fingerprints,” of ozone change that, according to current understanding, can be uniquely associated with a specific cause.
- Identify the roles of human activity, solar cycle variations, and other undetermined natural variability in altering stratospheric ozone.
- Evaluate the reliability of models for stratospheric ozone and their ability to predict change.

The development of two-dimensional (2-D) models of stratospheric chemistry and transport has led to considerable improvement in our ability to describe the stratosphere, to predict ozone distributions, and to compare with observations of ozone and other trace compounds (see *WMO*, 1986). Two-dimensional calculations allow us to simulate both the latitudinal and seasonal variations in the stratosphere, a task beyond the scope of the 1-D models traditionally used for assessment. Results from the 2-D models may allow for identification of fingerprints in ozone: i.e., certain months and latitudes for which chlorofluorocarbon (CFC)-induced ozone effects are most pronounced. We have chosen to base our present study on results from 2-D models. We have included for historical perspective some results from parallel 1-D models (from the same research groups as for 2-D models), but find that 1-D models cannot be used to predict even the globally averaged perturbations to ozone.

Although many features in these atmospheric simulations are common to all models, significant differences exist. There are systematic discrepancies in all of the models with regard to the absolute concentrations of ozone at the stratopause and the source of odd nitrogen in the lower tropical stratosphere. These stratospheric models represent the most recent versions available from the research groups involved, and thus are not fully or, in some cases, partly documented in the published literature. A detailed intercomparison of the 2-D models has not yet been made, but is planned for 1988. For these reasons, we have incorporated a brief section on comparison with observations and an extended discussion on uncertainties pertinent to the model calculations in this study.

## 7.1 ATMOSPHERIC SCENARIOS FOR 1955–1990

The period of focus for this study was selected to be the last 30 years, because there is an extensive data base collected on total column ozone by the Dobson network for this period, starting with the International Geophysical Year, 1957. Factors that could have influenced atmospheric ozone during this period include slow increases in the concentration of biogenic/anthropogenic trace gases such as carbon dioxide (CO<sub>2</sub>), methane (CH<sub>4</sub>), and nitrous oxide

## THEORY AND OBSERVATIONS

(N<sub>2</sub>O); a rapid rise in the concentration of stratospheric chlorine from the manmade gases CFCl<sub>3</sub>, CF<sub>2</sub>Cl<sub>2</sub>, carbon tetrachloride (CCl<sub>4</sub>), and methylchloroform (CH<sub>3</sub>CCl<sub>3</sub>); injection of nitrogen oxide (NO) by atmospheric nuclear tests; and variations in ultraviolet (UV) sunlight over the 11-year solar cycle. These terms have been included in the model scenarios selected here. Other geophysical factors that lead to noticeable changes include changes in tropospheric chemistry and climate, increases in brominated halocarbons, volcanos, heterogeneous chemistry in the polar stratosphere, and changes in circulation associated with the quasi-biennial oscillation (QBO) and the El Niño/Southern Oscillation (ENSO). The neglect of these latter terms is discussed with the uncertainties in the models. Table 7.1 indicates the combinations of factors that are incorporated in the different calculations.

In addition to the primary period, 1955–1985, we believe it is important to extend the calculations through 1991 in order to predict near-term global trends in ozone as we approach the next maximum in the solar cycle. A realistic assessment of the predictions of ozone change is needed since, according to current theory, increases in ozone caused by increasing solar intensity could fully or partially cancel the calculated ozone decreases caused by the effect of trace gases, as described below.

**Table 7.1** Factors Included in Model Simulations

Case	CFC's	N <sub>2</sub> O & CH <sub>4</sub>	solar	nuclear	T & CO <sub>2</sub>
1	yes	yes	no	no	(some)
2	yes	yes	yes	no	(some)
3	yes	yes	yes	yes	(some)

Case 1 illustrates the effects of changes in trace gases only. In case 2, the effects of the solar cycle are introduced through cyclic changes in the solar ultraviolet (UV) flux. In case 3, releases of NO from atmospheric nuclear tests during 1958–1962 are included. Changes in stratospheric temperature will be driven by changes in CO<sub>2</sub> and O<sub>3</sub>; some of the models were able to include this feedback, others were not (see model description below).

### 7.1.1 Trace Gases

Emissions and atmospheric concentrations of important trace gases, such as CO<sub>2</sub>, CH<sub>4</sub>, N<sub>2</sub>O, and several chlorocarbons, are known to have increased substantially over 1955–1985. Scenarios for the historical variations in these gases are based on observed increases in concentrations or on estimates of the emissions of these gases (Wuebbles et al., 1984), as outlined in Table 7.2. The scenarios employed here represent one possible reconstruction of the recent composition of the atmosphere. Nevertheless, the uncertainties in the trace gas composition of the atmosphere over

**Table 7.2** Trace Gas Scenarios Adopted for 1950–1991

CO <sub>2</sub> (ppm)	$270 \times (1.00141)^{(t-1950)}$	$t < 1958.0$
	$270 + 44.4 \times (1.0192)^{(t-1958)}$	$t > 1958.0$
CH <sub>4</sub> (ppm)	$0.70 + 0.93 \times (1.018)^{(t-1980)}$	$t < 1980.0$
	$1.63 \times (1.010)^{(t-1980)}$	$t > 1980.0$
N <sub>2</sub> O (ppb)	$285 + 14.0 \times (1.041)^{(t-1978)}$	all t

Concentrations refer to bulk tropospheric values; t is time in years. Based on fits supplied by D. Wuebbles (see Wuebbles et al., 1984).

the last three decades are bounded by measurements, and alternate scenarios that are consistent with observations would not produce significantly different results in these models.

Yearly release rates of chlorocarbons are given in Table 7.3 for each year between 1955 and 1985. Fluxes of chlorocarbons are assumed to be constant after 1985. Other trace gases, such as CO and NO<sub>x</sub> (=NO + NO<sub>2</sub>), which may have had important effects on tropospheric ozone, are kept at a constant level, partly due to major uncertainties about their emissions over this time period and partly due to the uncertainties connected to the treatment of tropospheric chemistry in the present models. For example, aircraft emissions of NO<sub>x</sub> were not included; there are uncertainties in theoretical emission rates, in addition to uncertainties in how to model the tropospheric NO<sub>x</sub> and ozone (O<sub>3</sub>). Carbon monoxide (CO) increases are not considered, although there are indications that Northern Hemispheric levels have been increasing slowly (see Chapter 8). Halon (bromocarbon) scenarios were not included because the increase in

**Table 7.3** Fluorocarbon Emission Fluxes (10<sup>9</sup>g/yr) Used in Models for 1950–1991

Year	CFCl <sub>3</sub> (CFC-11)	CF <sub>2</sub> Cl <sub>2</sub> (CFC-12)	CHClF <sub>2</sub> (CFC-22)	C <sub>2</sub> Cl <sub>3</sub> F <sub>3</sub> (CFC-113)	CCl <sub>4</sub>	CH <sub>3</sub> CCl <sub>3</sub>
1955	21.5	46.9	0.6	0.0	91.0	3.4
1956	26.1	53.3	0.8	0.0	87.9	7.4
1957	31.3	60.5	1.1	0.0	84.8	16.4
1958	31.3	68.6	1.4	0.0	84.8	19.6
1959	31.3	77.9	1.9	0.0	84.8	23.3
1960	38.2	88.5	2.6	2.5	84.8	27.8
1961	47.3	100.5	3.5	3.0	84.8	33.0
1962	58.5	114.1	4.2	3.7	84.8	39.2
1963	72.4	129.5	5.1	4.4	88.7	46.6
1964	88.7	148.2	6.1	5.4	92.8	55.5
1965	100.8	167.6	7.3	6.5	97.0	65.9
1966	114.6	189.5	8.8	7.9	101.5	78.4
1967	130.2	214.3	10.6	9.6	106.1	93.2
1968	148.0	242.4	12.7	11.6	111.0	110.8
1969	168.2	274.1	15.3	14.0	116.1	131.7
1970	191.2	300.5	18.3	17.0	121.4	156.6
1971	217.3	327.9	22.0	20.6	127.0	186.2
1972	247.0	357.9	26.5	24.9	132.9	221.3
1973	280.7	390.6	31.8	30.2	139.0	263.1
1974	323.5	443.5	38.3	36.6	145.3	312.8
1975	323.5	434.6	46.0	44.3	131.2	371.9
1976	323.5	433.9	50.3	53.6	131.2	442.1
1977	325.5	418.0	55.0	65.0	131.2	454.5
1978	316.5	388.6	60.1	74.4	131.2	454.5
1979	307.8	388.6	65.7	85.1	131.2	454.5
1980	264.5	388.6	71.9	97.3	131.2	454.5
1981	264.5	412.2	71.9	97.3	131.2	454.5
1982	264.5	412.2	71.9	97.3	131.2	454.5
1983	264.5	412.2	71.9	97.3	131.2	454.5
1984	264.5	412.2	71.9	97.3	131.2	454.5
1985	264.5	412.2	71.9	97.3	131.2	454.5

## THEORY AND OBSERVATIONS

stratospheric bromine from manmade halocarbons is expected to have had only a minor effect on ozone through 1985. (A notable exception may be the polar ozone reductions, which are not addressed in these calculations.)

### 7.1.2 Solar Variability

Variations in sunlight over the 11-year solar cycle are believed to manifest themselves as cyclic changes in the solar flux on the order of 10 percent or less in the far ultraviolet, with very small changes, if any, in the visible region of the spectrum. The far UV—wavelengths less than 220 nm—is responsible for photolysis of O<sub>2</sub> and, hence, primary production of ozone. (Destruction of ozone is driven, in general, by wavelengths longer than 240 nm.) The maximum in solar UV is associated with the maximum of the solar cycle (defined by sunspot number or F<sub>10.7</sub> flux) and is expected to produce an increase in stratospheric ozone. The magnitude of the solar-cycle effect on ozone will depend on the amplitude and spectrum of solar variations as well as their impact on the distribution of other trace gases in the stratosphere.

The large solar-cycle model used here for variations in solar UV, shown in Table 7.4, is based on SBUV data and the analyses of Heath and Schlesinger (1984; 1986). A fundamental assumption for this model is that the spectral pattern of variability observed over the solar rotation of active regions (27 days) is the same as that over the solar cycle (11 years). The magnitude of the solar cycle in UV irradiance is assumed to scale linearly with the ratio of the core-to-wing emissions of the Mg II line. An alternative case for solar variability is the small solar-cycle model, presented in WMO (1986) and based on Solar Mesospheric Explorer (SME) observations. Lean (1987) notes that the solar variability derived from SBUV data is significantly higher than that derived from SME satellite data. Some 2-D model calculations also were made with this pattern for the solar cycle.

**Table 7.4** Assumed Peak-to-Peak Variation of UV Radiation During a Solar Cycle as a Function of Wavelength

Wavelength (nm)	Large* Model (%)	Small** Model (%)
175–190	12	2.0
190–210	10	3.0
210–240	4	2.6
240–260	3	0.5
260–300	1	0.5

\*SBUV

\*\*SME

In the present model studies, UV flux changes are represented by a simple sine curve through each solar cycle. This assumption ignores the asymmetry of the solar cycle observed in sunspots or F<sub>10.7</sub> flux, which exhibits a rapid rise to solar maximum and a slower decay to minimum. Variations in UV radiation that occur during a solar cycle are still highly uncertain. The magnitudes of individual solar cycles are based on solar radio emissions, F<sub>10.7</sub>, assuming the magnitude of solar cycle 21 (1974–1985) to be unity. All solar cycles are assumed to have the same baseline flux at solar minimum. Table 7.5 shows the amplitude of each solar cycle. In these model studies, it is assumed that solar UV variation is the only external variation associated with the solar cycle.

**Table 7.5** Relative Magnitude of Solar Cycles

Cycle No.	Year of Max.	Relative Magnitude
18	1946.5	0.89
19	1957.5	1.30
20	1968.5	0.86
21	1979.5	1.00
22	1990.5	1.00 (assumed)

Adopted from Heath & Schlesinger (1984), scaled to  $F_{10.7}$  flux.

### 7.1.3 Nuclear Test Series

In estimating the changes in ozone during the 1960's, it is necessary to include the impact of NO produced by the U.S. and U.S.S.R. nuclear test series of the 1950's and 1960's. Past modeling studies (e.g., Chang et al., 1979; Wuebbles, 1983b) have predicted that these tests would have significantly perturbed stratospheric ozone.

For our calculations, we have selected a limited set of nuclear tests, based on the more complete list of Bauer (1979). This subset, shown in Table 7.6, includes all explosions greater than or equal to 10 megatons (MT) and accounts for about 70 percent of the total megatonnage during the primary testing period in 1961 and 1962. A comparison made with a more complete compilation of the test series shows that the limited set is a good approximation. The altitudes of the bottom and top of the stabilized cloud are taken from the empirically based analyses of Peterson (1970) and assume a uniform source of NO (molecules/cm<sup>3</sup>) between cloud bottom and cloud top. The production of NO per megaton of explosion energy is still highly uncertain, with theoretical estimates ranging from  $0.4-1.5 \times 10^{32}$  (see discussion in Chang et al., 1979, or NRC, 1985). We assume here a value of  $1.0 \times 10^{32}$ . An exception to the above scenarios was the LLNL model which adopted a yield of  $0.67 \times 10^{32}$  NO per MT, and that used the altitude distribution of NO within the cloud from Peterson (1970).

The major uncertainties in simulating these nuclear tests are the yield of NO and the altitude range of the cloud, particularly for the high-latitude U.S.S.R. tests. The timing and yield (megatons) of the tests are well established.

**Table 7.6** Limited Set of Nuclear Tests Used in Model Calculations

Date	Country	Latitude	Yield(MT)	Alt (km) +
May 12, 1958	USA	11°N	1.4*	13-19
July 28, 1958	USA	11°N	8.9*	18-29
Oct. 23, 1961	USSR	75°N	25	19-37
Oct. 30, 1961	USSR	75°N	58	20-42
June 27, 1962	USA	2°N	11	18-30
Aug. 5, 1962	USSR	75°N	38	20-41
Sep. 19, 1962	USSR	75°N	24	18-36
Sep. 25, 1962	USSR	75°N	27	18-36
Sep. 27, 1962	USSR	75°N	24	18-36
Oct. 30, 1962	USA	17°N	10	18-30
Dec. 23, 1962	USSR	75°N	20	19-35

+ Altitude range (km) of the injected NO

\*Surface test

## THEORY AND OBSERVATIONS

### 7.1.4 Atmospheric Variations Not Modeled

When comparing the model simulations discussed above with observed values of total ozone for the same period, it is important to bear in mind that the ozone concentrations are also influenced by factors that are not considered in the models.

The atmosphere is variable on all scales, many of which cannot be resolved by our current models. For example, some of the variability in total ozone appears to be correlated with the QBO, but this atmospheric cycle has not been included in these ozone trend studies. The more regular annual and semiannual cycles are generally included in these models through the seasonal variation in sunlight (included directly in the photochemistry and indirectly through imposed atmospheric temperatures or transports). The annual cycle is large at high latitudes, and most models would capture this variation producing a spring maximum and fall minimum in total ozone (see Figure 7.3). There is also a semiannual component that has been investigated in some models.

The QBO is quasi-periodic, which complicates attempts to model it with regular, periodic functions. In addition, major climatic events, such as ENSO, are likely to affect the stratosphere and induce temporary changes in ozone. Other irregular phenomena include solar proton events that are erratic, that tend to occur on the waning side of the solar cycle, and that can produce large amounts of  $\text{NO}_x$  in the middle and upper stratosphere (Crutzen et al., 1975; Jackman et al., 1980).

More important, the 2-D model studies presented here did not attempt to simulate the large ozone decreases observed in the Antarctic spring over the last 8–10 years, nor to study the possible consequences of proposed Antarctic chemistry at other latitudes. The model calculations also do not consider the possible effects on stratospheric ozone and temperatures of the volcanic eruptions of El Chichón in April 1982 and Agung in 1963. All of these studies require special research efforts, many of which are in progress. Neglect of these irregular geophysical phenomena probably represents an important source of error in simulating the recent ozone trends.

## 7.2 THE MODELS

### 7.2.1 Model Descriptions

The present work is based on experiments with four different 2-D models (described in Table 7.7) and with some parallel 1-D models. With the exception of the LLNL 2-D model, they were all used in the previous compilation of model results. (See WMO 1986, Chapters 12 and 13, for a more complete description of the types of 2-D stratospheric models and their performance.)

Three of the 2-D models (AER, LLNL, and Oslo) use a diabatic circulation, although their transport velocities can differ because the circulations are derived from different data sets. In the AER and Oslo models, the circulation is fixed in all computations. In the LLNL model, the temperatures are held fixed, while the radiative heating rates and the diabatic circulation are computed as ozone varies. The fourth 2-D model (Cambridge) uses a Eulerian circulation. The mean transport by waves in the Cambridge model is represented as momentum fluxes based on satellite observations and specified diffusion coefficients, and is held fixed while changes in the

Table 7.7 Characteristics of 2-D Models Used in Calculations of Chapter Seven

	AER	Cambridge	Oslo	LLNL	LLNL
Dimensions	2-D	2-D	2-D	2-D	1-D
Model Domain and Resolution	Pole to Pole $\Delta \sim 9.5^\circ$ 0-55km $\Delta Z = 3\text{km}$	Pole to Pole $\Delta \sim 10^\circ$ 0-60km $\Delta Z \sim 3.5\text{km}$	Pole to Pole $\Delta = 10^\circ$ 0-50km $\Delta Z = 2\text{km}$	Pole to Pole $\Delta = 10^\circ$ 0-54km $\Delta Z = 3\text{km}$	0-56km $\Delta Z = 1\text{km}$
Circulation	Diabatic circulation based on prescribed temperatures and diabatic heating rates	Eularian circulation derived from calculated momentum fluxes based on satellite obs.; latent heat release; radiative transfer (self-consistent); and prescribed diffusion coefficients	As AER	Diabatic circulation radiative heating rates calculated self-consistently both for shortwave heating and longwave cooling	
Diffusion	Stratosphere Above 20mb: $K_{yy} = 3 \cdot 10^9$ Below 20mb: 30°S-30°N: $3 \cdot 10^9$ 30°-Pole: $6 \cdot 10^9$ winter $2 \cdot 10^{10}$ summer  $K_{zz} = 1 \cdot 10^3$ $\text{cm}^2\text{s}^{-1}$ , increasing above 40km (gravity waves) Troposphere $K_{zz} = 1 \cdot 10^5$ $\text{cm}^2\text{s}^{-1}$ $K_{yy} = 2 \cdot 10^{10} \text{cm}^2\text{s}^{-1}$	Luther's (1973) monthly averaged K values	Stratosphere $K_{yy} = 3 \cdot 10^9$ $\text{cm}^2\text{s}^{-1}$ $K_{zz} = 1 \cdot 10^3$ $\text{cm}^2\text{s}^{-1}$ , increasing above 40km (gravity waves)  Troposphere: $K_{yy} \sim 4 \cdot 10^{10}$ $\text{cm}^2\text{s}^{-1}$ $K_{zz} \sim 1 \cdot 10^5$ $\text{cm}^2\text{s}^{-1}$	Stratosphere $K_{yy} = 2 \cdot 10^9$ $\text{cm}^2\text{s}^{-1}$ $K_{zz} = 1 \cdot 10^3$ $\text{cm}^2\text{s}^{-1}$ , increasing above 40km  Troposphere: $K_{yy} \sim 1 \cdot 10^{11}$ $\text{cm}^2\text{s}^{-1}$ $K_{zz} \sim 1 \cdot 10^5$ $\text{cm}^2\text{s}^{-1}$	$K_z$ variable with altitude Wuebbles (1983b)
Surface Boundary Condition $\text{O}_3$	Fixed mixing ratio	Dry deposition	Dry deposition	Dry deposition	As 2-D
Chemistry	Oxygen, hydrogen, methyl, nitrogen, chlorine species  Tropospheric $\text{H}_2\text{O}$ specified by relative humidity  Diurnal calculations performed 10 timesteps per day, 5 timesteps per night	Oxygen, hydrogen, nitrogen, chlorine species, methyl chemistry parameterized  As AER  Diurnal averaged	Oxygen, hydrogen, methyl, nitrogen, chlorine, bromine species  As AER  Diurnal calculations performed once every month $\Delta t = 15$ min.	Oxygen, hydrogen, methyl, nitrogen, chlorine species  As AER  Separate diurnal calculations are used to derive rate factors for diurnal-averaged model	as 2-D  + bromine  As AER  As 2-D

## THEORY AND OBSERVATIONS

**Table 7.7 (Cont'd)** Characteristics of 2-D Models Used in Calculations of Chapter Seven

	AER	Cambridge	Oslo	LLNL	LLNL
Dimensions	2-D	2-D	2-D	2-D	1-D
Model Domain and Resolution	Pole to Pole $\Delta\phi 9.5^\circ$ 0-55km $\Delta Z = 3\text{km}$	Pole to Pole $\Delta\phi 10^\circ$ 0-60km $\Delta Z \sim 3.5\text{km}$	Pole to Pole $\Delta\phi 10^\circ$ 0-54km $\Delta Z = 2\text{km}$	Pole to Pole $\Delta\phi 10^\circ$ 0-54km $\Delta Z = 3\text{km}$	$\Delta\phi 10^\circ$ 0-56km $\Delta Z = 1\text{km}$
Photolysis	Calculated ~every hour 93-405 nm $\Delta\lambda = 5$ nm or less. Two-stream approximation Rayleigh scattering  Cloud albedo	Calculated 3 times per day 170-800 nm 171 intervals Parameterized Rayleigh scattering  No clouds	Calculated every hour 180-800 nm 130 intervals Two-stream approximation Multiple Rayleigh scattering ( $n = 3$ )  Cloud albedo	Calculated ~every 15 min. 133-735 nm 148 intervals Successive multiple Rayleigh scattering  Cloud albedo	As 2-D
Temperature Calculations	Temperatures fixed	Solving the thermodynamic equation	Changes in temperatures in the stratosphere calculated as $\Delta T = \Delta T_{\text{CO}_2} + \tau \cdot \Delta H$ where $\Delta^2 T_{\text{CO}_2}$ is a prescribed function of $\mu_{\text{CO}_2}$ (taken from the model of Lacis and Hansen (private comm.); the radiative damping time scale is prescribed and the change in the shortwave heating, $\Delta H$ , is calculated self-consistently with $\text{O}_3$ changes	Temperatures fixed	Radiative equilibrium temperatures in the stratosphere, calculated self-consistently
Solar Heating		$\text{O}_3$ and $\text{O}_2$ heating	$\text{O}_3$ , $\text{O}_2$ , and $\text{NO}_2$ heating	$\text{O}_3$ , $\text{O}_2$ , and $\text{NO}_2$ heating  Near IR heating from $\text{H}_2\text{O}$ , $\text{CO}_2$ , and $\text{O}_2$	As 2-D
IR Cooling		15 $\mu\text{m}$ $\text{CO}_2$ Curtis matrix 9.6 $\mu\text{m}$ $\text{O}_3$ cooling to space		Broadband model including $\text{CO}_2$ , $\text{O}_3$ , and $\text{H}_2\text{O}$	As 2-D
Literature References	Ko et al. (1985)	Harwood and Pyle (1975), Pyle (1980), Eckman, Haigh, & Pyle (1987)	Stordal et al. (1985), Isaksen and Stordal (1986b)	Wuebbles et al. (1987, in preparation)	Wuebbles et al. (1983a,b)

radiative transfer allow the circulation to change with ozone variations. The diffusion coefficients used for tracer mixing in the stratosphere are similar in the three diabatic circulation models, and generally larger in the Eulerian model.

All of the models are based on same chemistry (DeMore et al., 1985); however, the Oslo model is the only one to include bromine chemistry (held constant with time using background levels of  $\text{CH}_3\text{Br}$ ). All the models assume the same values for the solar flux and compute photolysis rates at a number of different times during the day. Various techniques are used to include the effect of diurnal variations in the chemical constituents.

Temperatures are calculated *ab initio* only in the Cambridge model, which calculates the temperatures from the thermodynamic equation. The AER and LLNL models keep the temperatures fixed in all computations. In the Oslo model, the temperatures in the stratosphere are allowed to diverge from a reference value, thus allowing for a temperature feedback to the chemistry. The assumption made in the Oslo model is that temperature changes are a purely radiative adjustment in response to changes in solar heating, while the diabatic circulation remains unchanged. There is some evidence for this assumption from the 3-D GFDL model (Fels et al., 1980). The LLNL model has employed the other extreme approach, namely that changes in the heating rates are manifested purely as dynamical adjustment to circulation.

### 7.2.2 Basic Chemical Uncertainties

Uncertainties in perturbation calculations that are due to known measurement uncertainties in reaction rate coefficients have been estimated for pure chlorine perturbations and for at least one combined perturbation (Stolarski and Douglass, 1986; Grant et al., 1985). An important result from such studies of error propagation is that combinations of rate coefficients that lead to a very high sensitivity of ozone to chlorine give poorer results in matching observed atmospheric constituents than do the models (i.e., combination of rate coefficients) with lower sensitivity to chlorine (Douglass and Stolarski, 1987). The conclusion reached in that study was that a combination of chemical reaction rate coefficients that yields a sensitivity of ozone to chlorine more than twice that calculated with the currently recommended rate coefficients is unsatisfactory. The conclusion rests upon chlorine monoxide (ClO) being the rate-determining radical for chlorine chemistry. The study is based on comparison of modelled and measured trace species at midlatitudes and, further, does not include the heterogeneous chemistry believed to be important in forming the Antarctic ozone hole.

Perhaps the most important facet of the chemical uncertainty is the question of completeness of the chemical mechanism. Early information on the atmospheric chemical mechanism was derived from relatively high-pressure laboratory experiments in which many reactions were occurring simultaneously. The reactions believed to be important were then isolated one at a time, and their reaction rate coefficients were measured. This process occurred over several decades of careful laboratory experiments. Our present atmospheric chemical scheme is constructed from these individually measured fundamental reaction rate coefficients.

In the early 1970's, many of the basic catalytic reactions had significant uncertainties in their reaction rate coefficients. Progress in laboratory kinetics caused rapid changes in the evaluation of perturbations. An example was the 1976 measurement of the  $\text{NO} + \text{HO}_2$  reaction, which found a rate coefficient more than an order of magnitude larger than previous values (Howard and Evenson, 1977). This led to model calculations of a lower stratosphere with significantly

## THEORY AND OBSERVATIONS

more hydroxyl radical (OH) in which chlorine-catalyzed loss of ozone becomes more important. It is now believed that uncertainties in most of the major catalytic reactions and radical-radical exchange reactions have been reduced to the order of 10–30 percent.

Another set of chemical uncertainties is associated with the major reservoir species such as chlorine nitrate (ClONO<sub>2</sub>). Much of the present uncertainty in the calculated sensitivity of ozone to chlorine or total odd-nitrogen (NO<sub>y</sub>) perturbations can be traced directly to the radical-reservoir balance, which is determined by the formation and destruction processes for the reservoirs. Many of the reservoir species are formed by three-body addition reactions, making their chemical impact greatest in the lower stratosphere and at high latitudes. These locations are shielded from UV radiation by ozone absorption, yielding significant reservoir molecule lifetimes, which in turn allow a buildup in their concentrations. The lower stratosphere and polar latitudes thus may be the regions of greatest chemical uncertainty.

More recently, the question has been raised as to whether there might be very slow reservoir-reservoir reactions that return two reservoir molecules to radicals, thus significantly enhancing radical chemistry and ozone destruction (WMO, 1986, Chapter 2). Laboratory experiments have shown that the homogeneous gas-phase rate coefficients for reservoir-reservoir reactions are insignificant, but the possibility remains of a significant heterogeneous contribution. This has, in fact, been suggested to be the mechanism for the rapid springtime change in Antarctic ozone (see, e.g., Solomon et al., 1986a; McElroy et al., 1986b; Isaksen and Stordal, 1986a; Crutzen and Arnold, 1986), where the surfaces for heterogeneous reactions are believed to be the polar stratospheric clouds (PSC's). New laboratory studies indicate that reservoir species containing chlorine are involved in this process. Observations of high ClO levels during periods with PSC's over Antarctica support this view (see the discussion in Chapter 11). The critical role of heterogeneous processes for Antarctic ozone chemistry is now emerging from a combination of atmospheric measurements, laboratory studies, and theoretical modeling efforts; but its importance for the rest of the stratosphere is still under debate. Of particular importance is understanding its role at high northern latitudes, where the meteorological patterns are quite different from those found over Antarctica, and also at all latitudes in the lower stratosphere after major volcanic eruptions.

As more and more laboratory studies are published, our confidence in the completeness of the chemical mechanism for stratospheric ozone has increased. Except for the effects of heterogeneous chemistry, the past 5 years have seen little change in the evaluation of specifically CFC perturbations.

### 7.2.3 Uncertainties in 2-D Model Transport

Significant advances have been made in the formulation of transport in 2-D models over the past few years. For instance, it has been shown that 3-D general-circulation models can be used to drive useful transport parameters for 2-D models (Plumb and Mahlman, 1987; Pitari and Visconti, 1985). Nevertheless, there are still many problems that could affect our ability to model changes in ozone: for example, only zonal mean processes can be explicitly described, and the transport changes slowly with season or with latitude. Unfortunately, we know that the atmosphere is highly variable on all scales. Data for trace gas distributions will reflect this variability; our models will not.

The rate of vertical advection coupled with the parameterization of eddy diffusion in the stratosphere determines much of the calculated distribution of the long-lived trace species. The

estimated distribution of methane is of particular importance for the partitioning of the chlorine species. A slow transport leads to lower concentrations of methane in the upper stratosphere, favoring a more efficient Cl/CIO formation and thereby a more efficient ozone reduction by catalytic chlorine reactions. Therefore, if the transport is too slow in the models, the chlorine effect is overestimated in the upper stratosphere. Comparisons of the calculated methane distribution with observations in some of the model studies indicate that this might be the case. However, the comparisons are not conclusive since the observations are also uncertain. SAMS measurements of methane indicate large latitudinal gradients in the upper stratosphere such that lower concentrations occur at higher latitudes. Models that duplicate this behavior (e.g., Solomon and Garcia, 1984a) and extend it to the polar regions (for which we are lacking observations) show a high sensitivity of ozone to chlorine in this region because of the relative absence of methane. This may be particularly important in assessing the latitudinal dependence of perturbations.

Furthermore, some of the processes influencing ozone on short time scales are inherently difficult to model within a 2-D framework. This applies especially to the kind of dynamical regime believed to exist in the Antarctic. An isolated vortex whose breakdown may well depend on ozone concentration is very difficult to model in two dimensions. Much of the transport description in 2-D models is empirical and thus does not allow the kind of feedback processes that may well be important in studying trends in ozone.

#### 7.2.4 Comparison of Models With the Contemporary Atmosphere

The credibility of stratospheric models in predicting future ozone change will depend on how well they reproduce current observations, particularly the distribution of key species directly involved in ozone chemistry. Such tests of the models allow for ready intercomparison of models and may help us understand any differences in the calculated scenarios for ozone, both past and future.

Because the chemistry of the stratosphere involves a nonlinear system of chemical reactions, one should expect the results of perturbation calculations to be sensitive to the initial chemical concentrations, in particular that of Cl<sub>y</sub> (total inorganic chlorine = Cl + CIO + HCl + HOCl + OCIO + Cl<sub>2</sub> + (CIO)<sub>2</sub> + ClONO<sub>2</sub>). This is especially true for the NO<sub>x</sub>-Cl<sub>y</sub> system, where the reaction of CIO with NO and the reaction of CIO and NO<sub>2</sub> to form ClONO<sub>2</sub> provide rapid transition between regimes dominated by Cl<sub>y</sub>- or NO<sub>x</sub>-catalyzed loss of ozone. This set of chemical reactions has been shown to result in a rapid increase in ozone sensitivity to chlorine at the level where Cl<sub>y</sub> is approximately equal to or greater than the total odd nitrogen concentration (e.g., Prather et al., 1984). For the current atmosphere, with Cl<sub>y</sub> levels well below NO<sub>y</sub> levels, the ozone depletion efficiency by chlorine reactions has been shown to increase with decreasing NO<sub>y</sub> levels. A model with initial low NO<sub>y</sub> levels tends to give greater ozone depletion from chlorine species than a model with high NO<sub>y</sub> levels (Isaksen and Stordal, 1986b). Thus, our assessment of the effect of simultaneous changes in a number of species in the stratosphere depends not only on the relative changes in each of the species, but also on the absolute concentrations of many key species.

We have here selected a few key species to characterize the behavior of stratospheric chemistry in the different models. Some of the models (Oslo, AER, and a previous version of the Cambridge model) have been involved in a comparison study earlier (WMO, 1986). It is not the objective here to make an extensive comparison of the different models used, but rather to apply

## THEORY AND OBSERVATIONS

the most recent versions of the models and point out where significant differences occur. To validate or to test more thoroughly these 2-D models, a more complete intercomparison of 2-D models is planned as a separate task in the near future.

### Ozone

All of the models show some of the main features common to the observed latitude–height distribution of ozone from the Limb Infrared Monitoring Spectrometer (LIMS) and the Solar Backscatter Ultraviolet (SBUV) (see Figure 7.1). Theoretical altitude profiles for the tropics are compared to a LIMS profile in Figure 7.2. The mixing ratio peaks above about 10 ppmv in the Tropics at about 34 km. The maximum calculated values range between 9 and 12 ppm in most models, (in reasonable agreement with the LIMS values). All models overpredict  $O_3$  at 30 km and underpredict it above 40 km. In the lower stratosphere, where ozone is controlled more by dynamical transport, the mixing ratio surfaces slope poleward and downward due to the predominant Brewer–Dobson circulation. In the models with the weakest horizontal diffusion (Oslo and LLNL), the slopes are steeper. In general, the models used here overpredict the peak mixing ratio of ozone, and some of them place the maximum mixing ratios below those observed by several kilometers.

There is a systematic discrepancy between observed and calculated ozone above 40 km, as discussed in WMO (1986). In the upper stratosphere, ozone is controlled by photochemistry, and the discrepancy might indicate some important errors in modeling stratospheric chemistry.

The integrated column abundance of ozone (often called total ozone) is shown in Figure 7.3 as a function of latitude and time of year. Figure 7.3 shows TOMS observations along with results from all of the models. The main features in the observations are adequately described by the models: low total ozone in the Tropics with little seasonal variation; increasing ozone column with latitude; a maximum in the Northern Hemisphere at very high latitudes in late winter; large seasonal variation at high latitudes; and a maximum in the Southern Hemisphere spring that occurs in midlatitudes rather than over the pole. The seasonal variation is suppressed in some of the models (AER and Oslo), yielding too-high ozone columns in the summer and fall. In the Southern Hemisphere, the maximum columns are observed at about 60°S in spring. While this

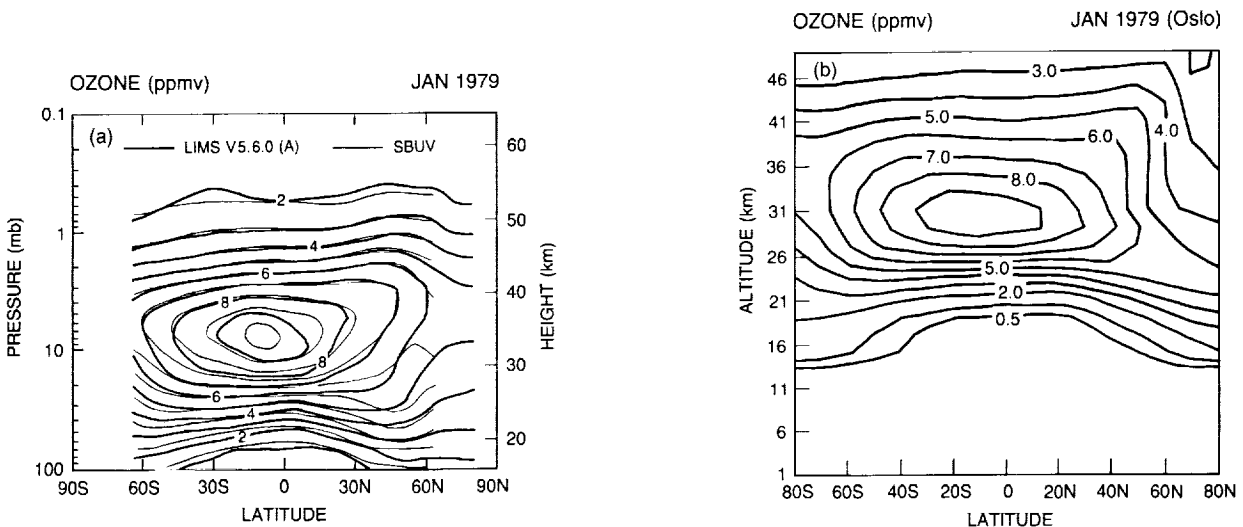


**Figure 7.1** Ozone-mixing ratio (ppmv) as a function of latitude and altitude for January from (a) LIMS and SBUV observations for 1979, (b) Calculations using Oslo 2-D model.

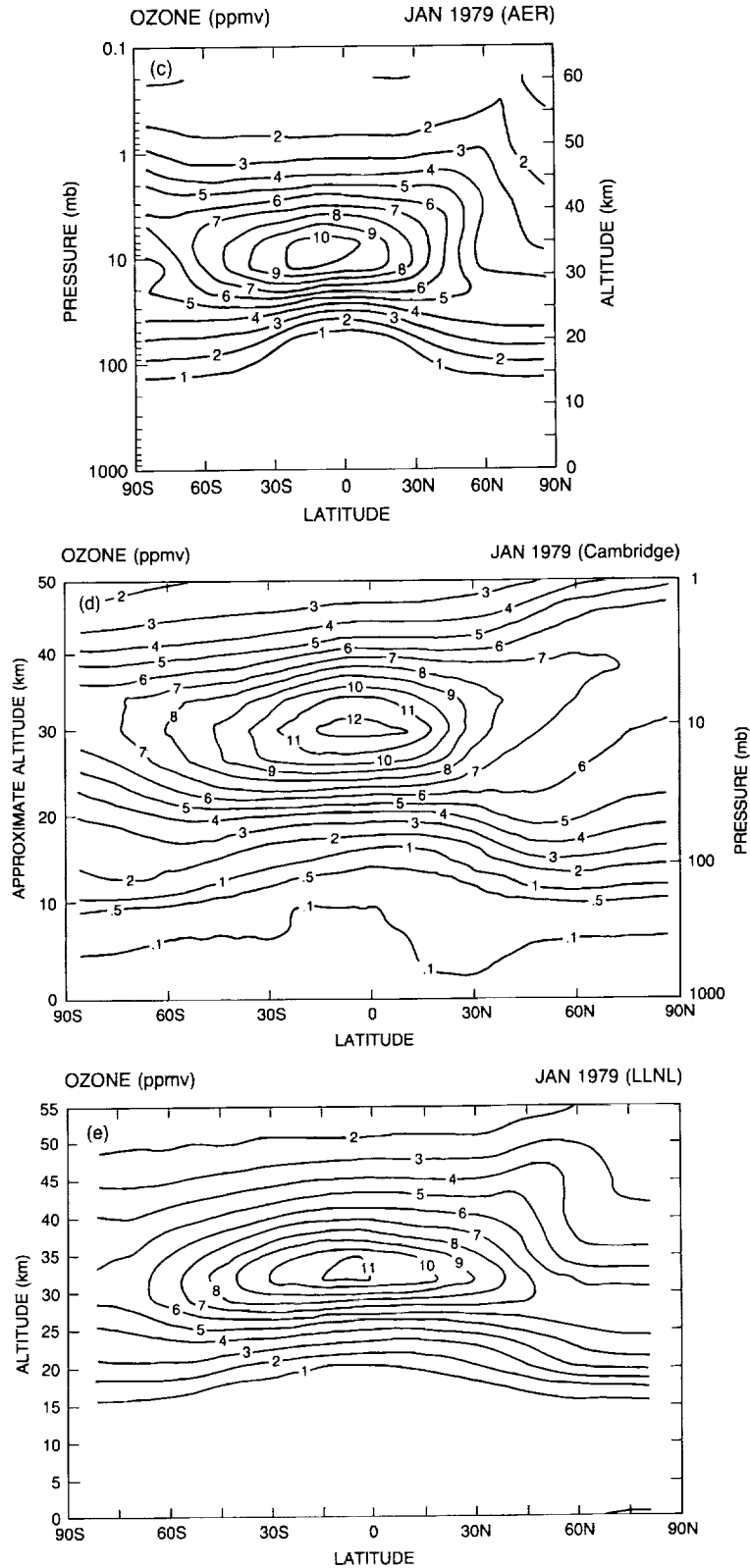


**Figure 7.1 (Cont'd)** Ozone-mixing ratio (ppmv) as a function of latitude and altitude for January from (c) Calculations using AER 2-D model, (d) Calculations using Cambridge 2-D model, (e) Calculations using LLNL 2-D model.

**THEORY AND OBSERVATIONS**

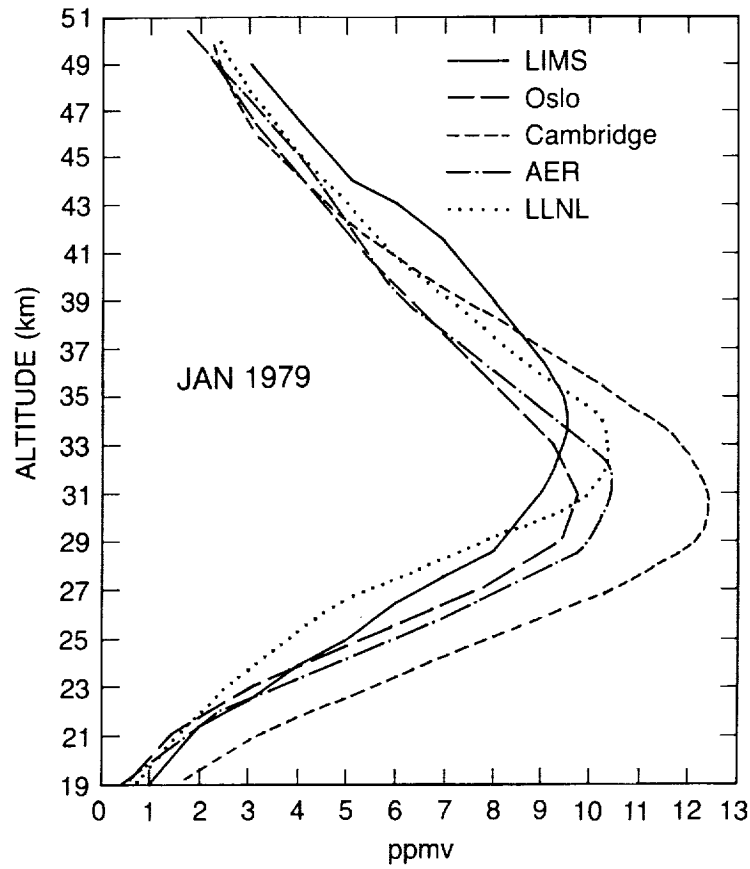


**Figure 7.2** Altitude profile of ozone-mixing ratios for January in the Tropics from LIMS observations and the four 2-D models.

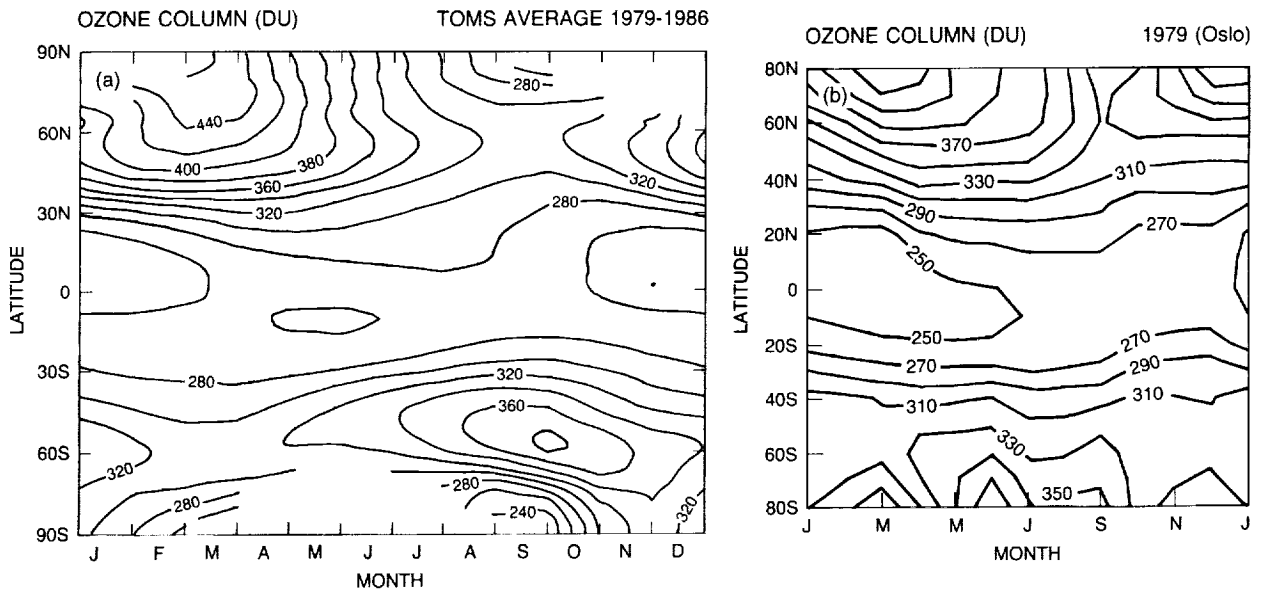


**Figure 7.3** Total column ozone abundance (Dobson Units) as a function of latitude and season for (a) TOMS observations averaged 1979–1986, and (b) the Oslo models.

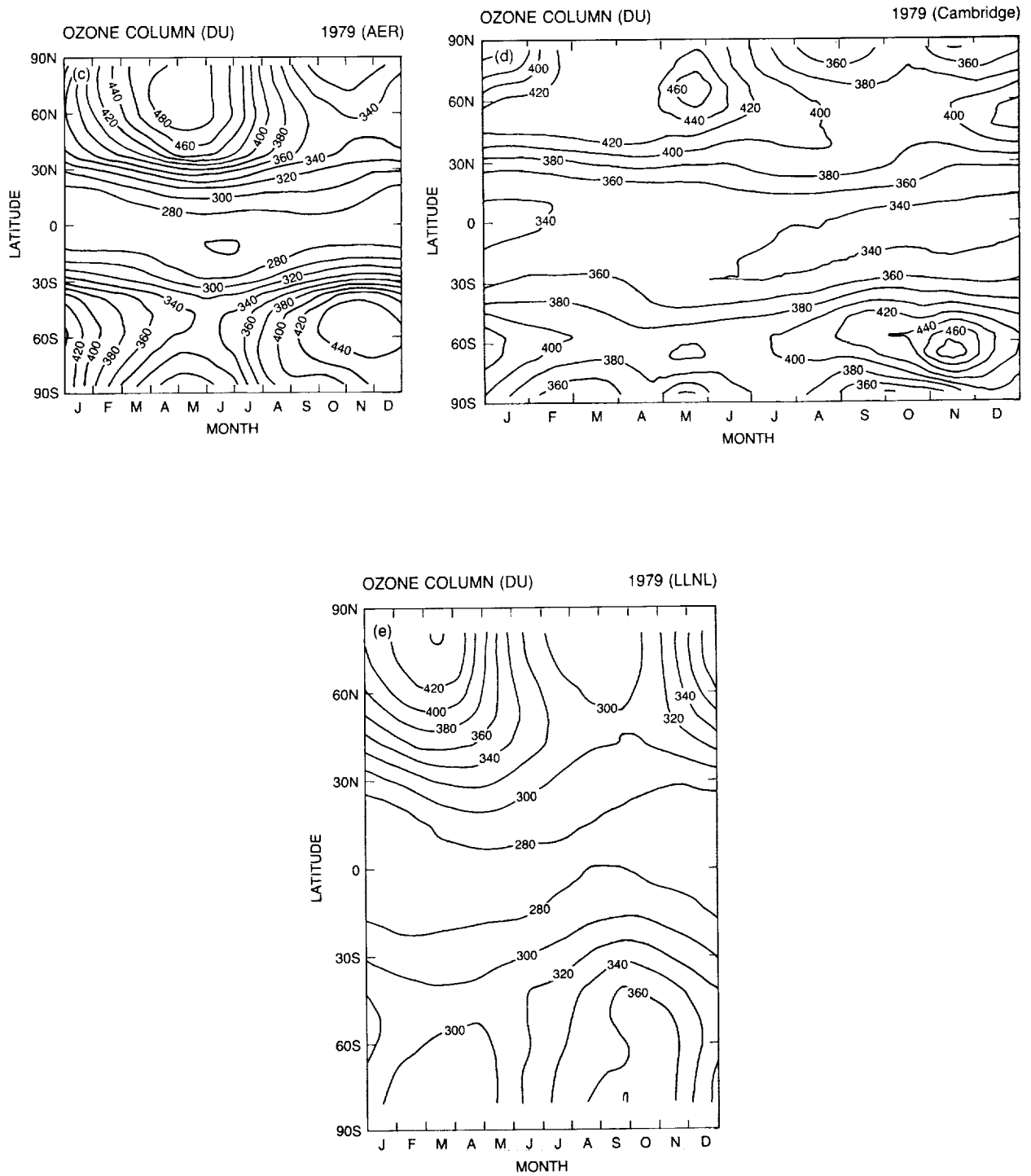


**Figure 7.3 (Cont'd)** Total column ozone abundance (Dobson Units) as a function of latitude and season for (c) AER, (d) Cambridge, and (e) LLNL models.

## THEORY AND OBSERVATIONS

maximum is found somewhat further poleward and later in the AER model, it is missing in the Oslo model (see discussion in Stordal et al., 1985). The Cambridge model, on the other hand, calculates ozone columns too high in the Tropics, as is expected from the high ozone mixing ratios in the middle and lower tropical stratosphere (Figure 7.2). In the Northern Hemisphere, the Cambridge model predicts maximum ozone columns at high latitudes during early summer, later than observed. As already mentioned, none of the models describes the Antarctic ozone hole, which is apparent in the Total Ozone Mapping Spectrometer (TOMS) data covering 1979–1986.

### *Odd Nitrogen ( $\text{NO}_y$ )*

One important issue brought up in previous 2-D model studies (WMO, 1986) was the apparent lack of agreement between models and observations of  $\text{NO}_x$  (LIMS observations of nighttime  $\text{NO}_2$ ), particularly in the tropical lower stratosphere. Models tended to underestimate the  $\text{NO}_x$  present in this region. Large uncertainties in the  $\text{NO}_x$  distribution strongly limit the models' ability to predict ozone distribution, as ozone production from the  $\text{CH}_4$ - $\text{NO}_x$  chemistry at these heights is very sensitive to  $\text{NO}_x$  levels. In the present diabatically driven 2-D models, additional  $\text{NO}_x$  is assumed to be produced by lightning, which is particularly efficient at high tropospheric altitudes. This source is shown to have a pronounced effect on  $\text{NO}_x$  levels in the upper troposphere and lower stratosphere in equatorial regions (Ko et al., 1986). Another possible mechanism that would increase  $\text{NO}_x$  levels in the lower tropical stratosphere is increased  $K_{yy}$  values, which would lead to increased transport of  $\text{NO}_x$  into the Tropics from midlatitudes.

Figure 7.4 is a latitudinal cross-section of  $\text{NO}_y$  at three different pressure levels—3 mb (~40 km), 16 mb (~30 km), and 30 mb (~25 km)—for July 1985. The figure shows that the present models (Cambridge model not shown) agree fairly well with the observed data. The modelled value for  $\text{NO}_y$  falls within the range of the data from LIMS and ATMOS (Russell et al., 1988). The  $\text{NO}_y$  maximum in the three models ranges from 21 to 23 ppb, which is within the uncertainty limits of the LIMS observations (Callis et al., 1985b).

The Oslo model has been used to study the impact of the lightning source of  $\text{NO}_x$  on ozone depletion. One scenario study has been performed both with and without the lightning source. In the case that involved changes in trace gases only, the depletion of globally averaged total ozone from 1960 to 1980 was reduced from -0.7 percent to -0.4 percent when a lightning source was introduced, as compared to a model without such a source; at the Equator, the ozone depletion changed from -0.7 percent to -0.3 percent. For the period 1960–1990, the calculated global decrease was reduced from -1.4 percent to -1.0 percent. At high latitudes, ozone depletion is less sensitive to these  $\text{NO}_x$  sources, decreasing from -2.1 percent to -1.9 percent (March). The uncertainties connected with the magnitude of the lightning source in the upper troposphere (source strength, conversion to and removal of nitric acid ( $\text{HNO}_3$ )) leads to additional uncertainties in these calculations.

In the present model simulations, one source of change in stratospheric odd nitrogen is included through the slow increase in the atmospheric concentration of nitrous oxide. Also included are the changes due to variations in UV radiation over the 11-year solar cycle. Several studies (e.g., Jackman et al., 1980; Garcia et al., 1984) have pointed out the potential for interannual as well as 11-year solar-cycle variations due to mesospheric and upper stratospheric production from energetic particles penetrating to these depths in the atmosphere. Callis and Natarajan (1986) claimed that a significant increase in odd nitrogen occurred as measured by SAGE-II in 1985 as compared to SAGE-I in 1979. Other observations so far have not confirmed the importance of such processes for variations in the ozone layer (see Chapter 9).

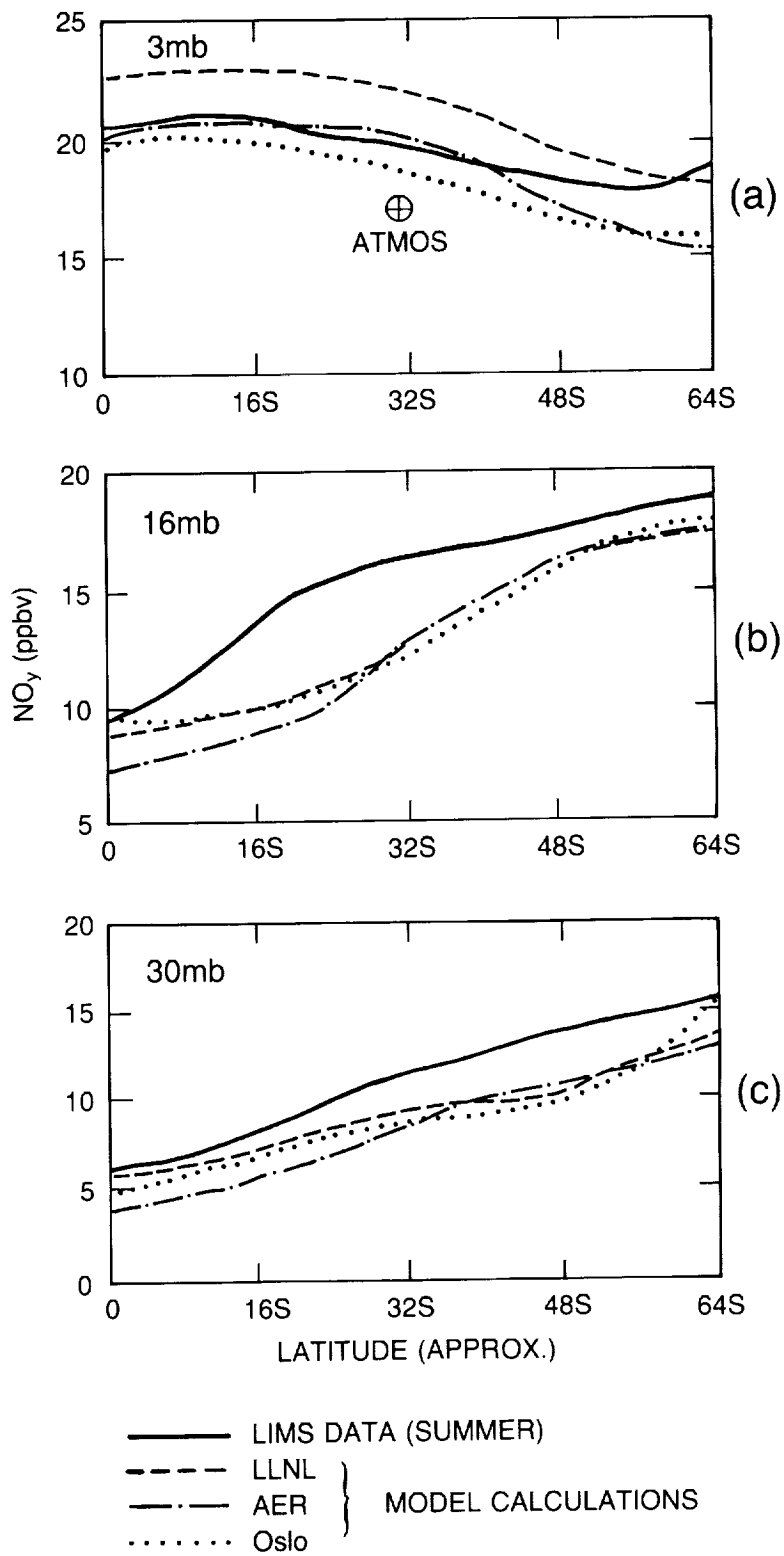


**Figure 7.4** Total odd nitrogen ( $\text{NO}_y$  in ppbv) as a function of latitude for summer from LIMS observations and from the four 2-D models for (a) 3 mb, (b) 16 mb, and (c) 30 mb. Also shown (crossed circle) are results from ATMOS.

**THEORY AND OBSERVATIONS**

*ClO*

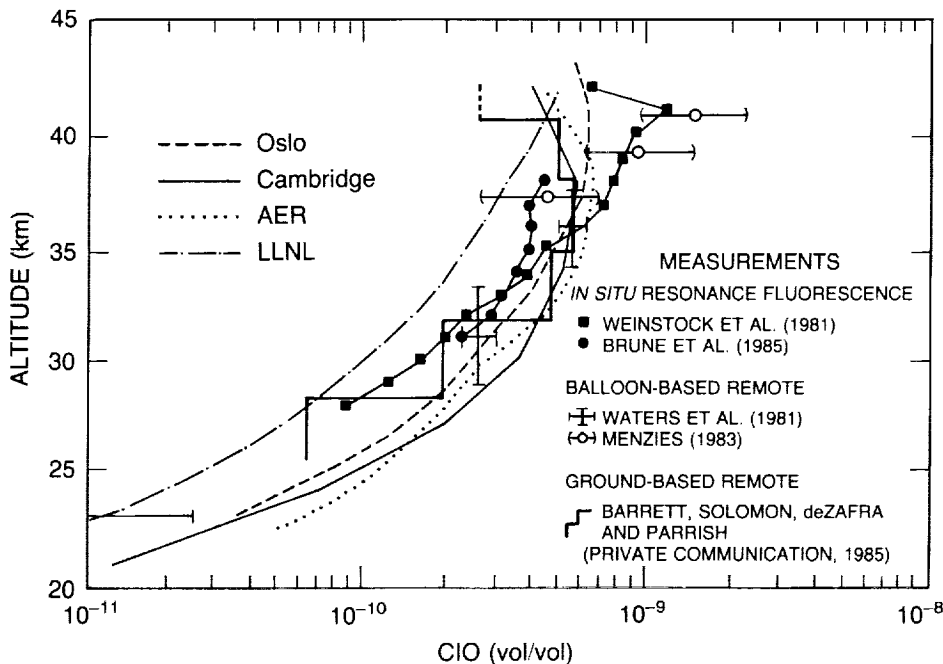
*ClO* is directly linked to ozone loss through the catalytic chlorine loss cycle. The ability of models to give a realistic description of CFC-induced ozone loss depends critically on their ability to give a proper description of the atmospheric behavior of *ClO* and its future change. Consequently, any noticeable differences in *ClO* distribution among the models could result in a different potential for ozone depletion.

Table 7.8 shows the  $Cl_y$  values in the upper stratosphere in 1960 and 1985. A general feature is that the absolute chlorine level in the contemporary atmosphere is dominated by recent releases of anthropogenically produced halocarbons. The main differences in  $Cl_y$  between models are a reflection of the differences adopted for background levels in 1960.

**Table 7.8** Total Chlorine Mixing Ratio ( $Cl_y$  in ppb) in the Upper Stratosphere at 30°N for July

	1960	1985	1985-1960
Oslo	0.9	2.4	1.5
AER	1.3	3.0	1.7
LLNL	0.9	2.6	1.7

Figure 7.5 shows the height profile of *ClO* (ppb) at 30°N during July 1985 for case 3, in which all effects are included. The vertical distributions of *ClO* at 30°N are similar in shape in all the models, but vary by more than a factor of two in concentration. As pointed out in WMO (1986), the model profiles are in reasonable agreement with the observations. Maximum *ClO* concentrations are predicted to occur around 40 km, with *ClO* levels between 0.5 and 1.0 ppb. The rapid decrease in mixing ratio below this altitude follows the observations quite well.



**Figure 7.5** Altitude profiles of *ClO* mixing ratio for July, 30°N, from measurements and from four 2-D models.

### 7.2.5 Stratospheric Temperature Feedbacks

The temperature of the stratosphere is predicted to respond to changes in ozone, to increases in CO<sub>2</sub>, and to volcanic aerosols, as well as to dynamical forcing through transport of heat. Over the study period, the past 30 years, model predictions indicate that stratospheric temperature changes associated with trace gases and the solar cycle are modest—a few degrees at most. These changes in temperature will feed back upon the chemical kinetics that control the concentration of ozone. The impact of including this feedback has been tested in the Oslo model. The 1979–1987 period corresponds to the most rapid decline predicted for ozone concentrations near 40 km. The estimated temperature decrease in the upper stratosphere is shown in Table 7.9 for the two solar-cycle cases over the 8 years. Inclusion of this decrease in temperature affects the predicted decline in O<sub>3</sub>, reducing the depletion by approximately 20 percent (see also Table 7.10).

**Table 7.9** Calculated Temperature Changes in 1985 vs. 1979 for Oslo Model, Case 3. Values Are Given for July at the Equator

Alt (km)	Large Solar Cycle Model	Small Solar Cycle Model
49	-2.40 K	-1.61 K
47	-2.86 K	-2.06 K
45	-2.94 K	-2.18 K
43	-2.84 K	-2.08 K
41	-2.15 K	-1.50 K
39	-1.44 K	-0.93 K
37	-1.30 K	-0.79 K
35	-1.10 K	-0.63 K

In the detailed comparison of the ozone simulations with observations, it may be important to include temperature changes caused by factors other than ozone. Temperature variations of a few degrees in the stratosphere due to year-to-year changes in dynamics or volcanic aerosols could have a significant effect on the modeled trend in ozone. The temperature record for this period is insufficient, however, and the model studies have not included this effect and its influence on ozone.

Estimated stratospheric temperature changes due to the increasing concentrations of CO<sub>2</sub> to date are small. Over longer time periods, however, looking into the next century, increases in CO<sub>2</sub> may have a more substantial impact on stratospheric temperatures. The effects of expected changes in tropospheric climate are not included in current stratospheric models and also may lead to uncertainties in the predicted temperatures of the stratosphere in the 21<sup>st</sup> century.

## 7.3 MODEL SIMULATIONS OF OZONE CHANGE

Calculations of the response of atmospheric ozone for the natural and anthropogenic variations described in Section 7.1 were made with the 2-D numerical models described in Section 7.2. The models were initialized with atmospheric conditions 1955 and integrated with time for the 30-year period of the study. One of the models (Oslo) continued calculations until 1991, the expected maximum of the upcoming solar cycle. The calculated history of ozone from the three cases defined in Table 7.1 is used to examine the relative contributions of the different geophysical forcings to changes in ozone over the study period.

## THEORY AND OBSERVATIONS

All experiments have been examined two dimensionally both in space (ozone mixing ratios as a function of latitude and altitude) and space-time (ozone columns as a function of latitude and time). In 2-D calculations, the effects of CFC releases might be easier to separate from natural variations in specific regions of the atmosphere during certain seasons when the maximum effects are calculated to occur (the CFC "fingerprint"). Most 2-D models indicate that ozone depletion, as reflected in total ozone observations, is most pronounced at high latitudes during the winter and spring seasons. This analysis focusses on the period 1979–1985 because of the ability to compare these calculations with available satellite ozone observations.

To understand the impact of the atmospheric nuclear test series, the latitudinal and global distributions of ozone during the 1960's are examined. Because the tests occurred at widely varying geographical locations, the previous 1-D model investigations of the response of ozone to nuclear tests would not have been adequate to define the latitudinal variation of the calculated response. Of particular interest are the high-latitude tests, which would be expected to yield local perturbations not representative of a global-averaged response. The perturbations introduced by the atmospheric bomb tests are expected to be negligible a few years after the bomb tests are stopped; thus, changes after the late 1960's come from the response to solar UV variations and possible changes induced by man's releases of trace gases (e.g., CFC's).

### 7.3.1 Calculated Total Global Variations

As discussed in Section 7.1, four 2-D models were used to simulate expected ozone variations since 1960. Figure 7.6 shows the calculations from each of these models for the three cases given in Table 7.1. The model calculations are shown as percent deviations of the total column of ozone from the 1970 value. All four models show similar decreases for perturbation case 1 (trace gases only). The ozone change for this case is smooth, with a decrease of nearly 1 percent reached by 1985 as compared to 1970. The initial decay in the AER model from 1960 to 1965 is a transient, due to the start of the calculations in 1960 rather than 1955. The other models began their calculations prior to 1960, and no transients from the initial condition appear in 1960.

The superposed solar cycle in perturbation case 2 has an amplitude of 1.5–2.0 percent in each model, all of which used the large solar-cycle model (Heath and Schlesinger, 1984) defined in Table 7.4. Use of the small solar-cycle model deduced from the Solar Mesospheric Explorer (SME) measurements (also Table 7.4) leads to a solar-cycle-induced amplitude somewhat less than half of that shown in Figure 7.6 (0.7 percent for the Oslo model).

The atmospheric nuclear tests of the early 1960's are superposed in Figure 7.6 for perturbation case 3. These occurred at a time of minimum expected ozone during the solar cycle. The bomb effects are predicted to have disappeared by the late 1960's.

Also shown for comparison to these globally integrated 2-D models are results for perturbation case 1 (trace gases only) for the AER 1-D model. That model was run for exactly the same conditions as the 2-D counterpart. The 1-D model shows considerably less ozone depletion since 1970, -0.2 percent at most. Similar differences between 1D and 2-D models are observed in the LLNL models. Thus, we find that 1-D models *cannot* be used to calculate even the globally averaged change in stratospheric ozone.

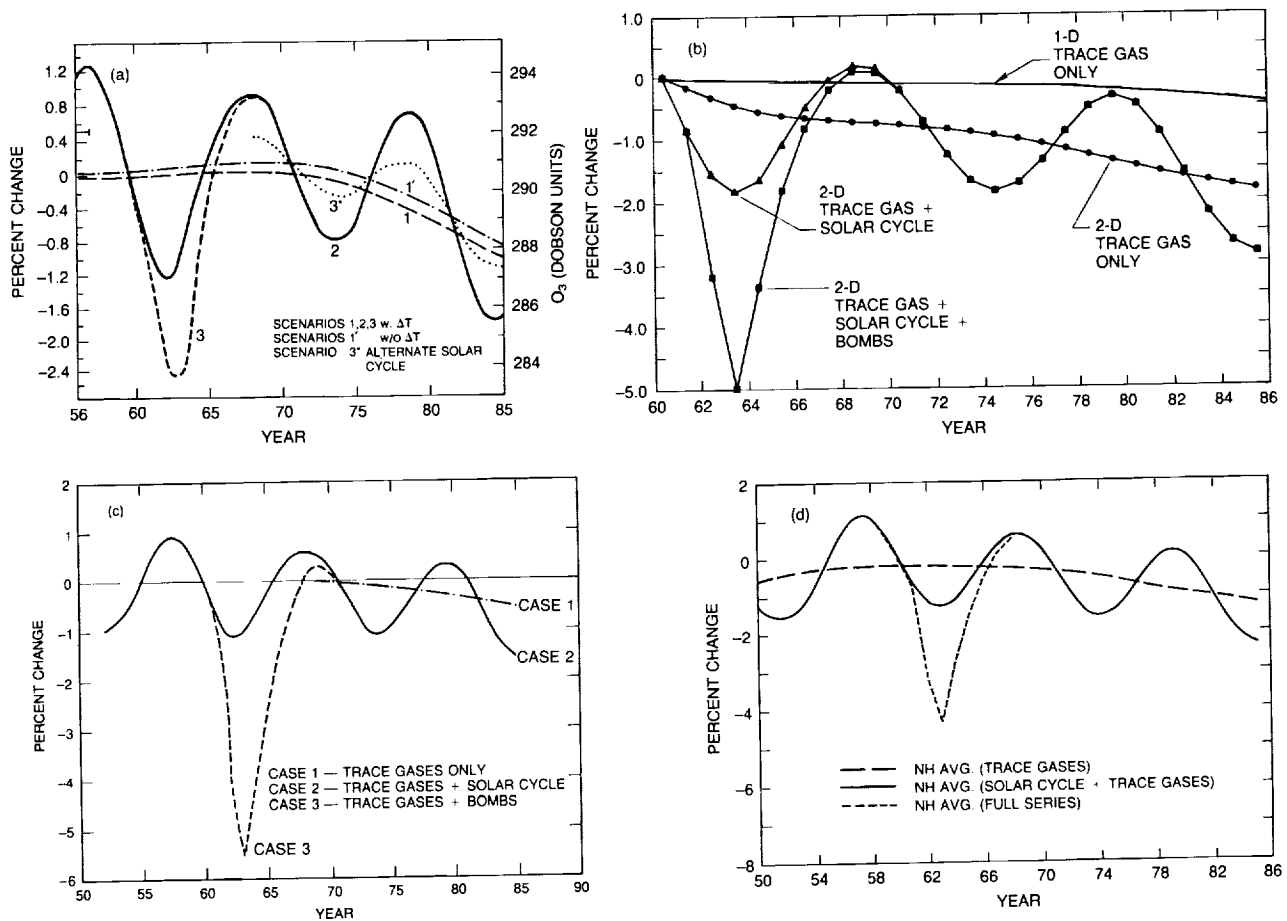


**Figure 7.6** Timeline of percent change in globally averaged column ozone from model calculations for the three cases described in Table 7.1: (1) trace gas emissions only, (2) trace gases plus solar cycle, and (3) trace gases, solar cycle, and atmospheric nuclear tests for the (a) Oslo, (b) AER, (c) Cambridge, and (d) LLNL models.

### 7.3.2 Atmospheric Nuclear Tests

The nuclear bomb tests during the late 1950's and early 1960's, with their associated injection of large amounts of nitrogen oxides into the stratosphere, provide a possibility of testing some aspects of the chemistry/transport models of the stratosphere. The model simulations of this period are based on the emission scenarios given in Section 7.1.3. As seen in Figure 7.6, all four models show a substantial depletion of total ozone during the year following the large explosions in late 1962. The globally averaged decrease was substantially different in the four models, with maximum yearly decreases ranging from 1.3 percent (Oslo) to almost 4.5 percent (Cambridge). The probable cause of this difference is the transport formulation in the models, since the bomb tests are predominantly released at high northern latitudes. Figure 7.7 shows total ozone depletion following the bomb tests in 1962 with time and latitude as calculated by the LLNL model; the model estimates total ozone to have dropped by 56–68 DU (Dobson Units) at 70°N.

A depletion of similar magnitude has been reported for observations of total ozone from the Dobson network (Reinsel, 1981; Angell et al., 1985; Bojkov, 1987) (see Figure 7.10). However, the observed depletion tends to start well before the time predicted by the models. This discrepancy

## THEORY AND OBSERVATIONS

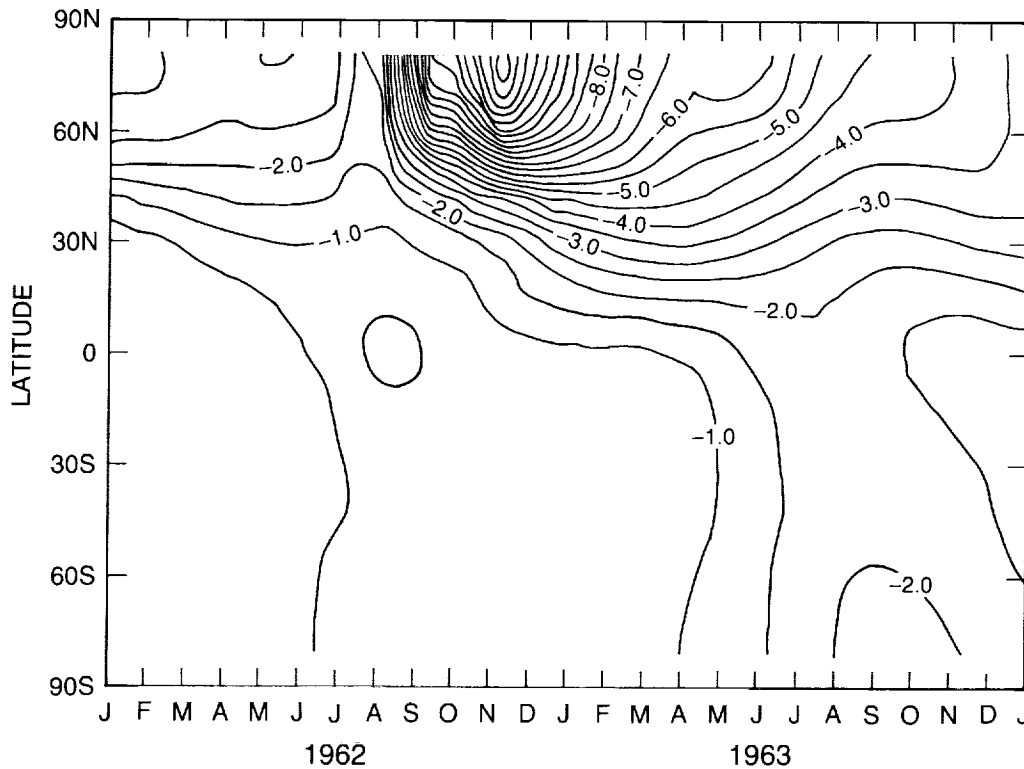


**Figure 7.7** Calculated change (%) in column ozone changes as a function of time and latitude during the atmospheric nuclear tests. Results from the LLNL 2-D model are shown for 1962–1963.

could have many causes, including the limited geographic representativeness of the early Dobson network. Until the reasons for the discrepancy are better understood, it is difficult to draw conclusions from this comparison regarding the ability of the models to simulate the atmospheric test series.

We have studied the sensitivity of the above results to moderate differences in the scenario for NO generated by the atmospheric nuclear tests. The difference between a simulation using the reduced set of bomb tests (Table 7.6) and one using the full set, including the smaller bombs, is of the order of 10 percent for the Northern Hemisphere average, the full set giving the larger depletion (LLNL model). A similar comparison using the Oslo model yielded even smaller differences. Based on these considerations, we estimate that the bomb tests are likely to have produced an ozone depletion at high northerly latitudes in early 1963 of 25–75 DU. The corresponding range for the global average depletion is 3–15 DU. These estimates should be regarded as tentative, as there still are uncertainties connected to the models.

The absolute magnitudes of the calculated ozone depletion depends, among other things, on the adopted emission scenario for NO. The assumption of  $1 \times 10^{32}$  molecules of NO produced by each MT total yield of nuclear explosion, as used in the AER, Oslo, and Cambridge simulations, is probably uncertain by at least a factor of two (see discussion in Section 7.1.3).

As seen in Figures 7.6 and 7.7, the recovery time of the depletion following the major explosions is a few years. Five years after the major injection in late 1962, very little depletion remained. This is a feature common to all models.

### 7.3.3 Column Ozone: Comparison With Observations

The primary long-term data set that is available for comparison to model calculations is that for total ozone from the ground-based Dobson spectrophotometers. Approximately 30 years of data can be used for trend analysis. Satellite data give a better global coverage of ozone distribution but are available only from late 1978. In the following sections, ozone trends calculated with the four 2-D models will be compared with ozone trends deduced from the Dobson network. An example using data from the TOMS instrument on Nimbus-7 will also be used for comparison. The emphasis of these studies is to search for fingerprints from theoretical models that can use existing measurements to separate the changes due to solar cycle from those due to trace gases.

#### 7.3.3.1 Theoretical Fingerprints for Solar Cycle and Trace Gases

We present two separate model calculations covering the period from solar maximum in 1979 to solar minimum in 1985: solar-cycle effects and concurrent changes in trace gases.

Calculated ozone changes due to solar-cycle effects alone are shown in Figure 7.8 for one model (Oslo), using the large solar-cycle case in Table 7.4. The main feature, which is the same for all four models, is the almost constant depletion of ozone with latitude and season ranging from 1.7 percent to 2.1 percent (Oslo model) going from solar maximum to solar minimum. For the small solar-cycle case, the Oslo model calculates ozone reductions of similar pattern, but smaller magnitude—about 0.7 percent.

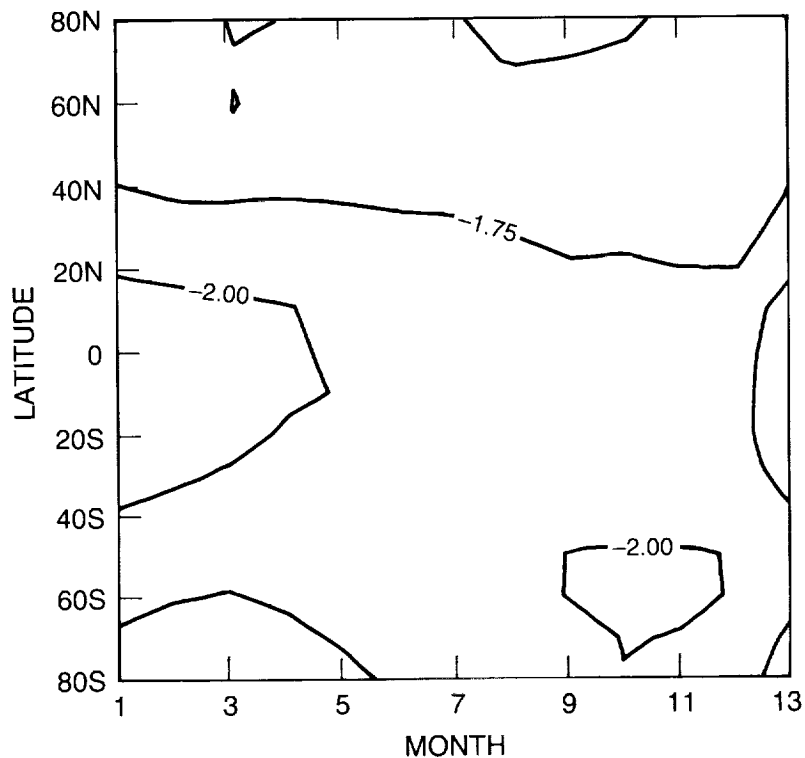


**Figure 7.8** Calculated change (%) in column ozone from 1979–1985 as a function of latitude and month from the Oslo model. The results demonstrate the effect of solar cycle (maximum to minimum) alone, neglecting all other influences.

**THEORY AND OBSERVATIONS**

The calculation for the same period, but with only trace gas changes included (case 1), is shown in Figure 7.9. In contrast to the solar cycle case, all the models show distinct latitudinal and temporal patterns of ozone depletion, with the largest changes occurring at high latitudes during winter and spring (n.b., results from the Cambridge model were not available for this figure; the Cambridge model is known to produce a quite different pattern at high latitudes for trace-gas impacts on ozone). However, the magnitude of the depletion, a global average of order 0.3 to 0.6 percent over this period, is substantially less than that obtained for the solar-cycle

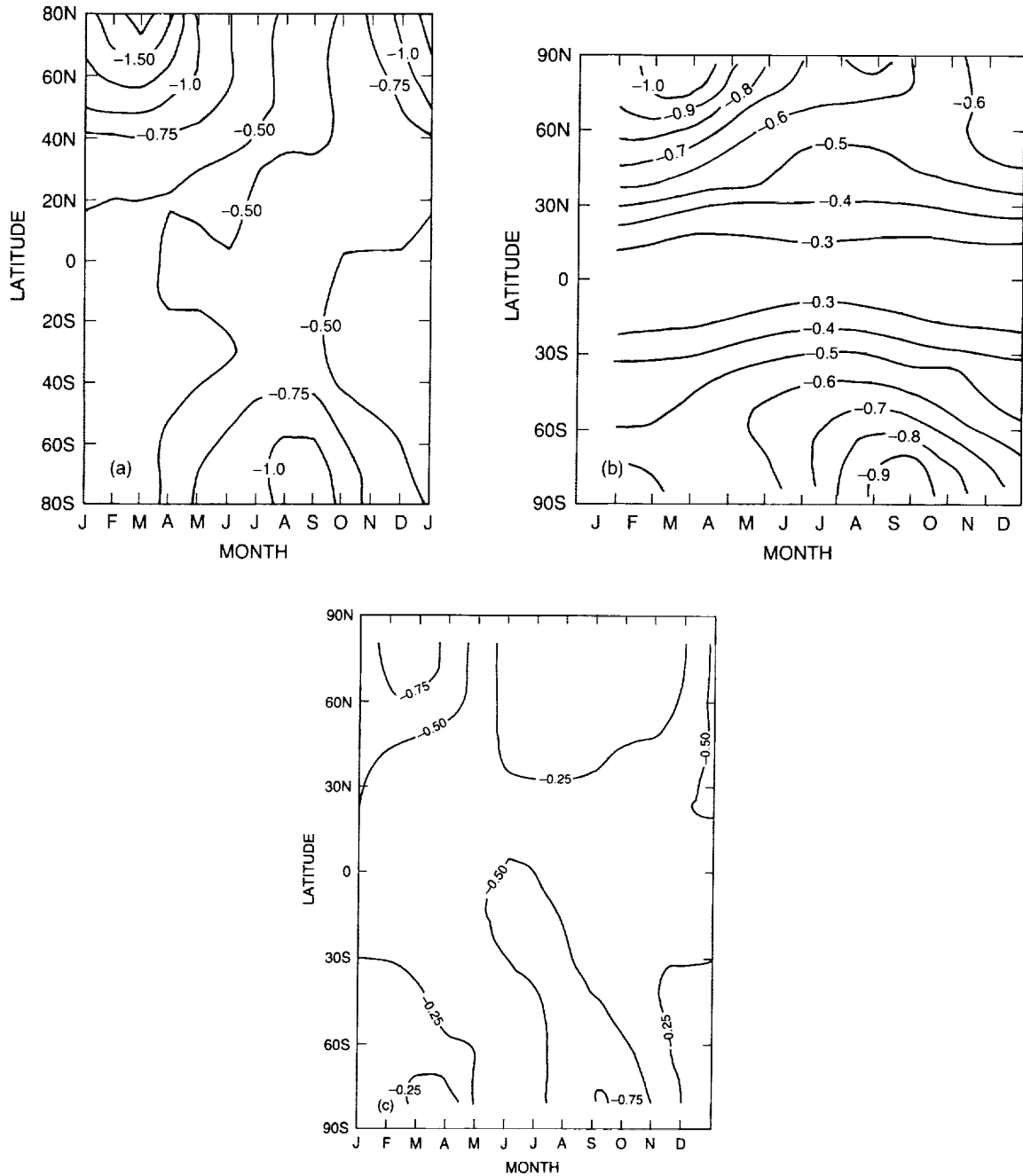


**Figure 7.9** Calculated change (%) in column ozone from 1979–1985 as a function of latitude and month, considering trace gases only (case 1). Calculations are from the (a) Oslo, (b) AER, and (c) LLNL models.

effects in the large solar-cycle case. If we compare with the case for small solar-cycle variations, then trace gases become more significant, particularly at high latitudes.

The magnitude and phase of the solar cycle must be correctly taken into account in data analysis for comparison with the models. For example, results from the AER model showed that shifting the time period for comparison by 1 year (1978 to 1984) led to noticeable changes in the calculated solar-cycle impact. Our current model for the solar-cycle variations is simplistic (a sine curve), and future efforts will require a more realistic model scaled to solar activity, such as the 11-year pattern for sunspots or 10.7 cm flux.

### 7.3.3.2 Thirty Years of Dobson Data

Thirty years of total ozone observations have been reanalyzed by Bojkov (1987) and presented in Chapter 4 of this report. The data have been divided into latitude bands, based on station location. The three latitude bands for which there were sufficient data to construct a meaningful average are shown in Figure 7.10 (30–39°N, 40–52°N, 53–64°N). For each of these latitude bands, calculations from the four models are superposed.

The observations show a distinct biennial oscillation, which is particularly pronounced at high latitudes. This feature is not seen in the calculations for reasons that already have been discussed. Also, there is an apparent solar-cycle variation that is broadly in agreement with the calculated solar-cycle variation. However, any trends related to trace gas releases are difficult to deduce from Figure 7.10 due to the large variability of the observations.

### 7.3.3.3 Global Data From Satellite, 1979–1987

A characteristic of the Dobson data presented for latitude bands in Figure 7.10 is its variability on all time scales. Much of this variability is meteorological and can be removed by the more complete coverage of satellite data available from late 1978. Even when satellite data are used to integrate over large areas of the globe, however, significant variability remains. Figure 7.11 shows one example using data from the TOMS instrument on Nimbus-7. The dots are the daily values of the area-weighted integral of total ozone from 65°S to 65°N over the 9-year data record. The point values are relative to the 9-year average for that particular week; the line through the points is a 60-day running mean. Also shown by a heavy line is the annual average calculated by the Oslo model, including both solar cycle and trace gas effects. The TOMS result is similar to that previously presented by Heath (1988) for SBUV data, except in this case, the TOMS data have been corrected as a function of time over the 9-year period by adjusting to the Dobson record (i.e., using satellite overpasses and subtracting the mean difference between the two records). As can be seen in the figure, the long-term changes in total ozone calculated by the model are in general agreement with observations, but the data exhibit significant variability relative to the long-term changes. It is not clear whether we should regard this failure to reproduce the observed variability as a fundamental discrepancy between models and theory or, more likely, as an inherent limitation in the 2-D nature of the models.

Additional information can be obtained from the seasonal and latitudinal behavior of the change in total ozone, as shown in Figure 7.12 for TOMS data, where the difference between the mean of the years 1985 plus 1986 and the mean of the years 1979 plus 1980 is plotted. The data have been adjusted to account for the drift of TOMS with respect to Dobson overpasses. The springtime Antarctic ozone hole is clearly visible, with changes of greater than 30 percent (see

## THEORY AND OBSERVATIONS

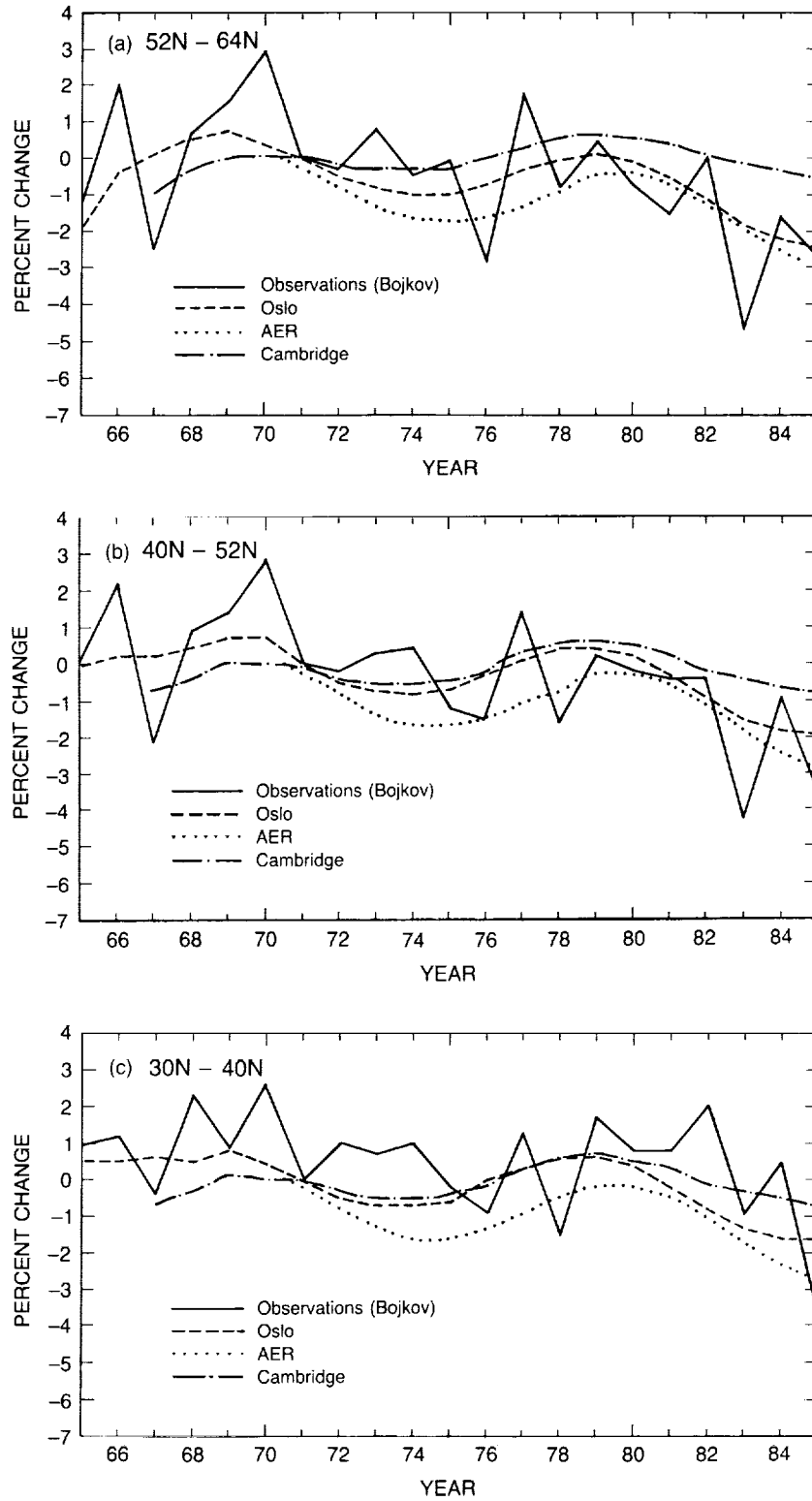


**Figure 7.10** Timeline of percent change in column ozone from 1965 to 1985 for the latitude bands (a) 52–64°N, (b) 40–52°N, and (c) 30–40°N. Reevaluated data from the Dobson network (see Chapter 4) are shown by the thick line. Calculations from three models (Oslo, AER, and Cambridge) are also shown for comparison.

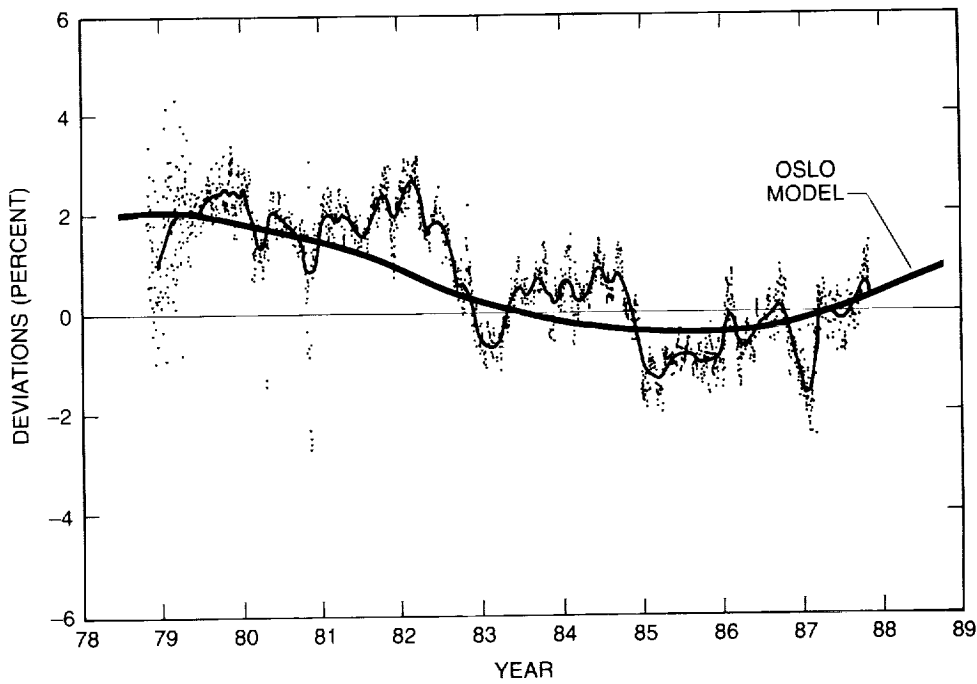


**Figure 7.11** TOMS data for column ozone integrated from 65°S to 65°N are shown for 1978–1987. The TOMS satellite data have been normalized to the ground-based Dobson network. The points represent percent deviations of the daily average from the 9-year average for that particular week; the thin solid line is a 60-day running mean through the points. The thick solid line shows calculated total ozone (Oslo model) for this period.

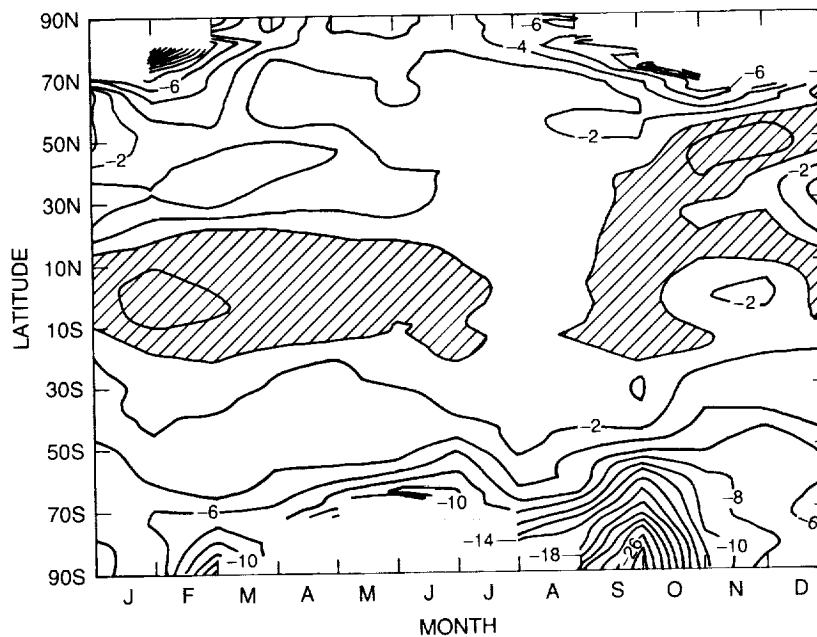


**Figure 7.12** Observed change (%) in column ozone from TOMS data, the average of 1985–1986 minus the average of 1979–1980. The TOMS data have been recalibrated and do not reflect the currently archived data: TOMS data for 1985 and 1986 have been increased by approximately 4 percent to account for drift with respect to Dobson network.

## THEORY AND OBSERVATIONS

Chapter 11). In addition to this primary signal, the data also show noticeable depletions at high latitudes in late fall, winter, and early spring. This pattern is closer to the calculated fingerprint for trace gases than it is to that for the solar cycle (see Figures 7.8 and 7.9). There is a possible indication from these TOMS data that the magnitude of the decrease in the winter at high latitudes may be more pronounced than that calculated in the models.

Calculations of the combined effects of trace gases and solar cycle from 1979 to 1985 are shown in Figure 7.13 as a function of latitude and season. The predominant change is a global net

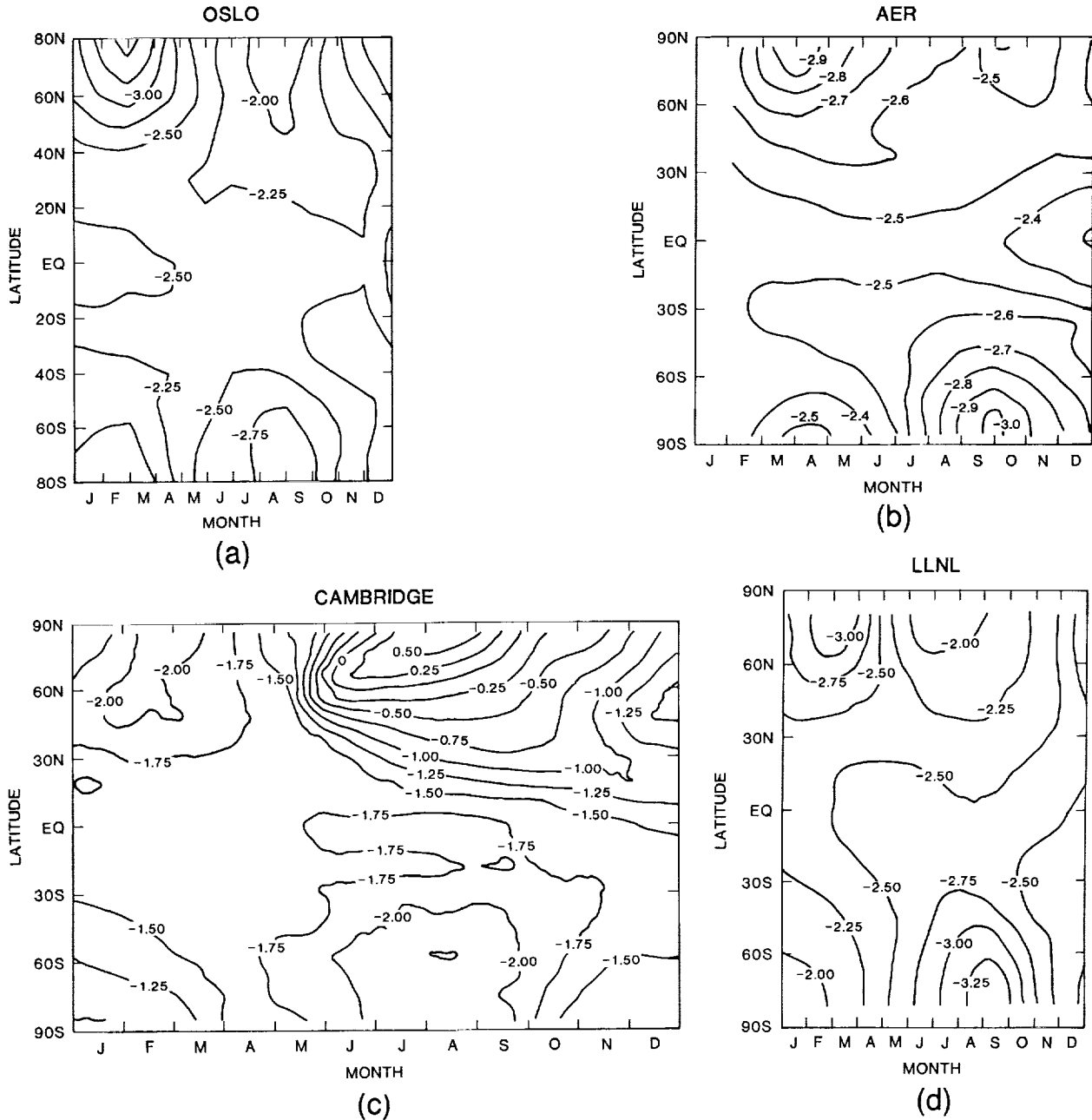


**Figure 7.13** Calculated change (%) in column ozone as a function of latitude and season from 1979–1985, including effects of trace gases and solar cycle. Calculations are from the (a) Oslo, (b) AER, (c) Cambridge, and (d) LLNL models.

decrease of order 1.5 to 2.5 percent that is associated with the solar cycle, and a smaller influence of the trace gases that is superimposed. Three of the models show similar variations, with largest decreases at high latitudes during winter, but the Cambridge model gives a markedly different result with ozone increases as large as 0.5 percent at high latitude during summer. The cause of this difference is not yet understood.

### 7.3.3.4 Subtracting the Solar Cycle From Dobson Data

One way to separate the solar cycle and trace gas effects is to use the Dobson data over two complete 11-year solar cycles. Bojkov (1987) in Chapter 4 has done this by comparing the records during two different seasons for two 11-year averaging period: 1965–1975 and 1976–1986. Figure 7.14 shows the difference between these 11-year records for the summer season (May–August) and the winter season (December–March) from each of 36 stations that are plotted as a function of station latitude. The summer season differences are small and consistent with the two model calculations, also shown in Figure 7.14. Decreases during the winter season are pronounced, and generally much larger than the model predictions, particularly north of 30°N. Model calculations

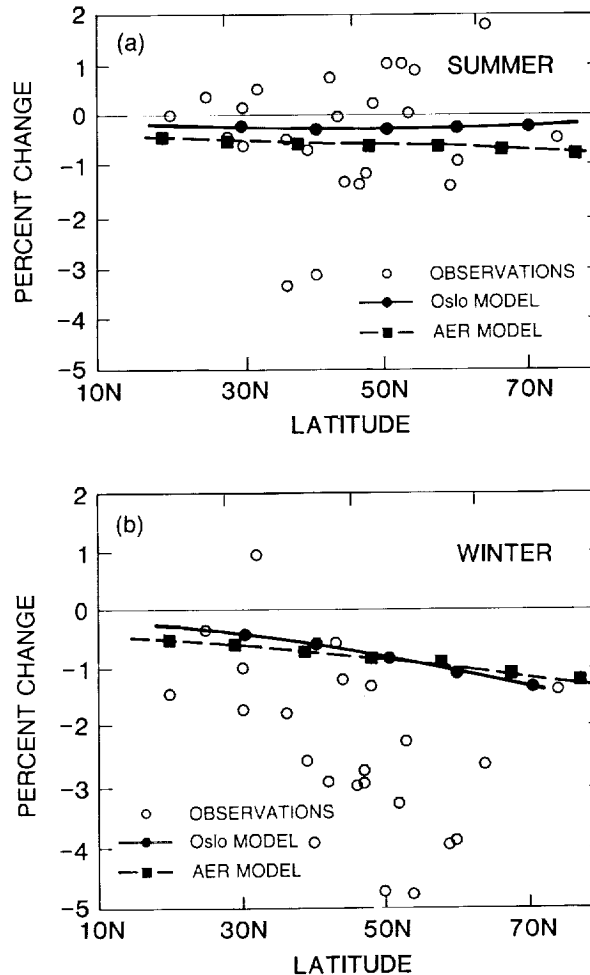


**Figure 7.14** Observed change (%) in column ozone between the 11-year (solar-cycle) averages 1965–1975 and 1976–1986 for (a) summer season (May–June–July–August) and (b) winter season (December–January–February–March). Points representing values from single stations are plotted as a function of station latitude. Results from two 2-D models (Oslo and AER) are also shown.

## THEORY AND OBSERVATIONS

(AER and Oslo) are in qualitative agreement with observations in that depletion increases toward higher latitudes, but the magnitude of the decrease predicted near 50°N (about -1 percent) is substantially less than that observed (about -1.5 to -4.5 percent).

If the similar feature seen in the TOMS data for 1979–1986 is robust (i.e., survives the current recalibration of the data set), then it is likely that current 2-D models underestimate the decreases in total ozone that have occurred at high northern latitudes over the last one to two decades. It is difficult at present to explain the cause of this discrepancy; however, it may be that the present 2-D models are missing some chemical processes, quite possibly heterogeneous chemistry that is particularly important at high northern latitudes, similar to that associated with the Antarctic ozone hole.

### 7.3.4 Profile Ozone: Comparison With Observations

We now examine the model-calculated changes in the local concentrations of O<sub>3</sub> as a function of latitude and altitude; we hope to associate different patterns of change with the geophysical forcing included in the models: trace gases, solar cycle, and atmospheric nuclear tests. This analysis will concentrate on the calculated differences between 1979 and 1985 (solar maximum to solar minimum). For this period, we have global data from satellites (SAGE-I and SAGE-II, SBUV) and limited coverage from ground-based observations (Umkehr). We focus on small percent changes in the vertical profile of ozone concentrations and look for latitudinal effects.

#### 7.3.4.1 Fingerprints of the Solar Cycle and Trace Gases

Ozone perturbations induced by the solar cycle alone (1979–1985, maximum-to-minimum, no trace gas changes) as calculated by the models are shown in Figure 7.15a as a function of height and latitude. Solar flux changes for the large solar-cycle model are used in these calculations. The decrease in UV intensities leads to decreases in stratospheric ozone at all latitudes and altitudes. The models predict a broad maximum around 40 km, with ozone changes between -1.5 and -3.0 percent. Calculations with the small solar-cycle model give a similar pattern, but with substantially smaller ozone perturbations. A characteristic pattern for the solar-cycle-induced changes is that the latitudinal gradients are moderate at all altitudes.

The calculated changes in O<sub>3</sub> concentrations between July 1979 and July 1985 for case 2 (trace gases plus solar cycle) are shown in Figure 7.15b–e for all four models. Ozone changes in the upper stratosphere (1–3 mb, 48–40 km) are dominated by the effect of chlorine increases rather than solar cycle (compare Figure 7.15a with 7.15b). The effect of trace-gas changes has a pronounced latitudinal pattern and is approximately twice as large as that from the solar cycle. Maximum depletion of ozone occurs about 2 mb (43 km) and ranges from  $-7 \pm 2$  percent in the Tropics to  $-10 \pm 2$  percent at mid- and high latitudes. From 1979 to 1985, the models predict decreases in *stratospheric* ozone at almost all latitudes and altitudes, the one exception being the Cambridge model, which predicts increases in the high-latitude lower stratosphere during summer. The upper stratosphere is, therefore, an area where the impact of CFC's can be more readily detected, as the trace-gas effects dominate the solar cycle for the period 1979 to present.

Results from all models show similar morphology in the upper stratosphere, although there are some differences near the winter pole. These variations may indicate the different way in which models treat the chemistry near the polar night, or may reflect differences in stratospheric transport at high latitudes. The magnitude of the maximum calculated change is almost twice as large in polar regions relative to the Tropics in three of the four models, whereas the LLNL model

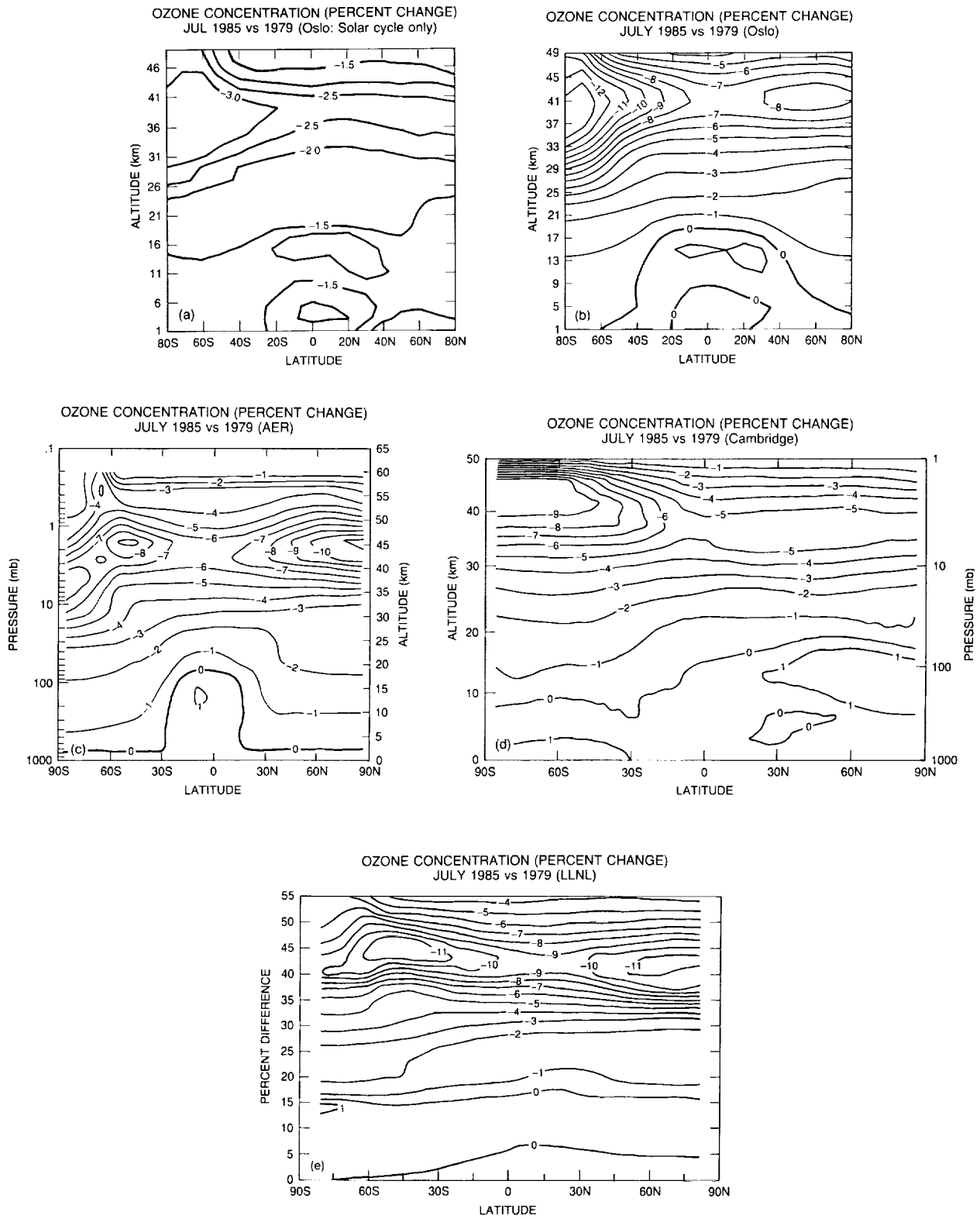


**Figure 7.15** Calculated height-latitude changes (%) in ozone from July 1979 to July 1985 for solar cycle only from the Oslo model (a), and solar cycle plus trace gases (case 2) from the (b) Oslo, (c) AER, (d) Cambridge, and (e) LLNL models.

## THEORY AND OBSERVATIONS

shows smaller latitudinal gradients at the altitude of maximum depletion (43 km). This latitudinal gradient in ozone depletion is, in part, a reflection of the relative distribution of ClO and CH<sub>4</sub>. The ratio of ClO to CH<sub>4</sub> increases toward high latitudes in the upper stratosphere, making the chlorine-catalyzed destruction of ozone more efficient.

In the lower stratosphere and troposphere, calculated ozone changes are small and show different patterns among the four models. Changes to ozone in the lower stratosphere dominate the perturbations to the ozone column. Comparison of the model results with observations in the lower stratosphere are further complicated by the effects of annual, semiannual, and quasi-biennial oscillations, which are not included in any of the simulations.

In the troposphere, calculated ozone changes are small and also show significantly different patterns among the four models. In general, ozone concentrations increase in the troposphere, although the pattern is quite different among the models and the magnitude is much less than that reported from analysis of the limited data base of tropospheric measurements (see Section 7.3.5). The predicted changes to tropospheric ozone would have little influence on the changes in the ozone column, but increases as large as +10 percent over this period (as reported by some analyses) could alter the total column ozone by as much as +1 percent.

Systematic changes in stratospheric temperatures over 1979–1985 would affect the calculated change in ozone. For example, an increase in stratospheric temperatures tends to increase the efficiency of photochemical loss of ozone and thus reduce ozone concentrations. The temperature may change due to variations in solar heating (proportional to ozone concentrations), in the radiative cooling of other trace gases, or in the dynamical transport of heat. The primary change in temperature over this period as calculated by the current models is a major reduction throughout most of the upper stratosphere (30–50 km) in response to the reduced ozone concentrations and, hence, reduced solar heating. The reduction in temperature calculated by the Oslo model partially offsets the ozone depletion in the upper stratosphere, reducing the magnitude by approximately 20 percent (see Table 7.10).

Previous analyses of Umkehr data for the 1970's have reported statistically significant decreases in upper and middle stratospheric ozone during this period (Angell and Korshover, 1983b; Reinsel et al., 1984). Observations indicate a maximum ozone reduction of the order of 3–4 percent in Umkehr level 8; most of the Umkehr stations used in the data analysis are located between 30–50°N. Results from three models (Oslo, AER, and LLNL) for 1970–1981 are shown in Table 7.10 for comparison. The calculated values are from case 1 (trace gases only) for 40°N and Umkehr layers 5 through 9.

**Table 7.10** Calculated Trends in Ozone at Umkehr Levels 5–9 for 1970–1981; Trace Gas Scenario Only

Umkehr Level	Oslo (T feedback)	Oslo (T fixed)	LLNL (T fixed)	AER (T fixed)
9	-6.5	-8.9	-9.3	-6.9
8	-6.8	-8.3	-11.0	-7.0
7	-3.7	-4.2	-4.9	-3.1
6	-1.5	-1.5	-1.5	-1.2
5	-0.5	-0.5	+0.2	-0.5

Results are for case 1 (trace gas only).

Results from the different models compare well in the lower layers, but there is a significant difference in layers 8 and 9, where the LLNL model gives the largest calculated change in ozone over 1970–1981. We are unable at present to explain these differences and await a more complete model intercomparison. Calculations with the University of Oslo model were done with fixed temperatures and with a parameterization for the change in temperature due to increased  $\text{CO}_2$  and changes in  $\text{O}_3$ . As noted above, temperature feedback is important in calculating ozone change, particularly in the upper stratosphere, layers 7, 8, and 9. Although in qualitative agreement with observations, all models give calculated changes in ozone in Umkehr levels 8 and 9 that are substantially larger than those determined from analysis of Umkehr data; the comparison is better at the lower levels.

All models show that the upper stratosphere is the altitude region most sensitive to trace gas releases, and that the magnitude of the effect exceeds effects introduced by solar-cycle variations. The models also predict strong latitudinal gradients due to increases in trace gases, in contrast to the impact of the solar cycle. Therefore, the upper stratosphere is the region where it should be possible to identify the fingerprints of trace gases on ozone. Such identification, however, will depend critically on the quality and global representation of the observations.

#### 7.3.4.2 Trends in Vertical Structure, 1979–1985

Figure 7.16 compares the changes in the altitude profile of ozone from SAGE-I (1979–1980) to SAGE-II (1984–1985, latitude belts 20°–50°N and 20°–50°S) and from the Umkehr network (stations

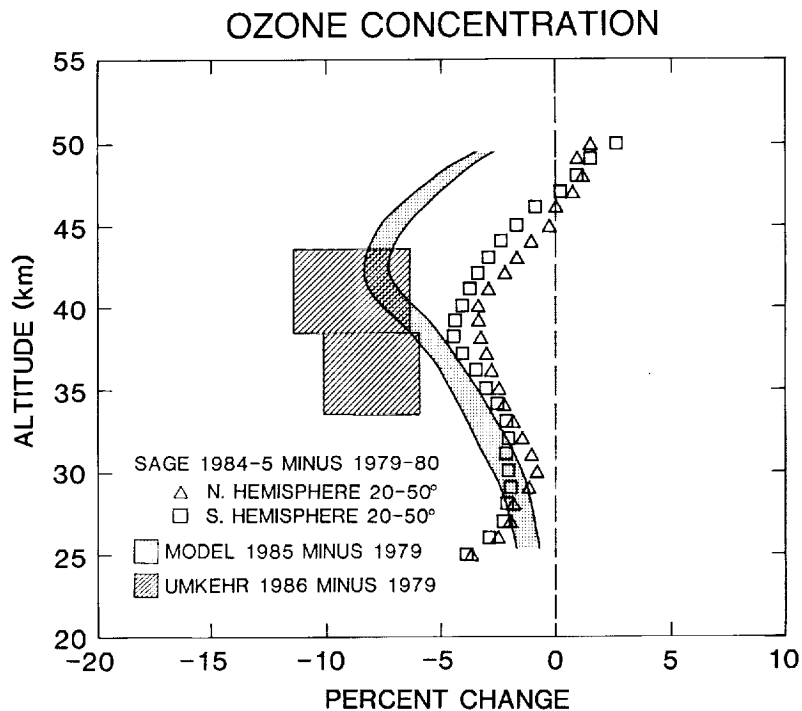


**Figure 7.16** Observed changes (%) in stratospheric ozone profiles from different instruments over 1979–1986. Differences between SAGE-I (1979–1980) and SAGE-II (1984–1985) measurements are shown for northern and southern latitudes (20°–50°). Umkehr observations from 1979–1986 are limited to northern midlatitudes. The band shows the range of model calculations (1979–1985, midlatitude, Oslo model) for both large and small solar-cycle models.

## THEORY AND OBSERVATIONS

between 36°N and 52°N) to the calculated change in ozone profile from the Oslo model (midlatitudes). Analysis of Umkehr data for trends during 1979–1986 is complicated by the strong interference of aerosols following the El Chichón eruption. One recent report, however, claims that it is possible to correct partially for this interference and, thus, to deduce upper stratospheric ozone changes over this period (see Chapter 5).

Both observations and models show ozone depletions that increase with altitude, peaking around 40–45 km. The calculated depletion in the upper stratosphere is larger than that reported from the SAGE observations, but slightly smaller than that from the Umkehr analysis. The discrepancy with the SAGE data is most pronounced around 50 km, where observations show a slight ozone increase. However, there is a possible systematic difference in derived ozone values between the two SAGE instruments that may be as large as  $\pm 4$  percent (see Chapter 5). The scale on the SAGE curve in Figure 7.16 could be shifted by as much as 4 percent, bringing the observations into better agreement with the calculations between 30 and 45 km, but still not explaining the small change above 45 km or the significant depletion below 30 km. Similarly enhanced ozone depletion in the lower stratosphere is deduced from ozonesonde data for the last two decades over Germany (Bojkov and Attmanspacher, 1988); however, changes of this magnitude in the lower stratosphere should be clearly evident in the total ozone column—and this is not apparent from the ozone column data.

The currently archived SBUV data for the same period show ozone depletions that are substantially larger than the models or data shown in Figure 7.16 and that have a distinctly different profile: a maximum ozone depletion of approximately 20 percent is found at 50 km. It is believed that these data cannot be used to determine changes in the ozone profile (see Chapter 5).

### 7.3.5 Tropospheric Ozone

#### 7.3.5.1 Impact on Column Perturbations

Although only about 10 percent or less of the total ozone column is located in the troposphere, increases in tropospheric ozone that have occurred over the last few decades might have produced a detectable change in the ozone column. Therefore, observed trends in total ozone must not be interpreted uncritically as reflecting stratosphere changes alone. Similarly, it is important for models to include tropospheric processes in a realistic way if they are to attempt to simulate changes in total ozone.

There are indications that the ozone levels in surface air are substantially higher in the present atmosphere over Europe and the U.S. than those found during the end of last century (Bojkov, 1986c; Kley et al., 1988), and that, during the last two decades, an increase of  $\sim 1$  percent per year has taken place in the free troposphere over most of the observing sites in the Northern Hemisphere (Bojkov, 1988b). Measurements over the last 30 years show substantial increases,  $\sim 50$  percent, during this period at surface levels over East Germany (Warmbt and Feister, 1984). The increases are not confined to the planetary boundary layer, but are observed also in the free troposphere. Ozone increases are observed to be largest northward of 40°N, with strong latitudinal dependence. Increases are particularly large over and around industrialized areas in Europe and North America (Logan, 1985). For example, ozonesonde observations over West

Germany (Bojkov and Attmanspacher, 1988) report increases much larger than 1 percent per year throughout the troposphere over the last 20 years.

Assuming that the reported increases in tropospheric ozone, ~1 percent per year, are representative of average conditions throughout the Northern Hemisphere for the last two decades, we can estimate the impact on the total ozone column. Tropospheric ozone should have produced an increase in column ozone of about 1 percent from 1970–1985 and about 0.5 percent from 1979–1985. Increases over industrialized areas would have been substantially greater, but these areas are a small fraction of the hemisphere. Therefore, the observed downward trend in total ozone at most northern sites might actually be larger than measured, being partially compensated for by increases in tropospheric ozone.

### 7.3.5.2 Uncertainties in the Estimates

The observed increase in tropospheric ozone is likely caused by anthropogenically induced increases in the concentration of precursor gases  $\text{NO}_x$ ,  $\text{CH}_4$ , nonmethane hydrocarbons (NMHC), and  $\text{CO}$ , although quantitative estimates are connected with large uncertainties (e.g., Isaksen and Hov, 1987). A main uncertainty in modelling tropospheric ozone comes from our lack of knowledge of  $\text{NO}_x$  distribution in the troposphere. Due to short chemical lifetime (days or less) and uneven source distribution,  $\text{NO}_x$  shows strong temporal and spatial variations in the troposphere. The efficiency of the  $\text{CH}_4$ – $\text{NO}_x$  chemistry for ozone production is strongly and nonlinearly dependent on  $\text{NO}_x$  levels, and the 2-D formulation of the current models is limited in representing the spatial variations in tropospheric  $\text{NO}_x$ . Additional uncertainties in ozone production and trends in the troposphere are introduced by our lack of knowledge of long-term trends in  $\text{CO}$ , NMHC, and  $\text{NO}_x$ .

The 2-D models used in this study all have a very crude representation of tropospheric processes. They do, in general, predict an increase in tropospheric ozone during the last two decades, but this increase is global and not limited to the northern midlatitudes, for which observations indicate substantially larger increases. Production of tropospheric ozone in the Northern Hemisphere may be underestimated because the models do not include any trends in short-lived anthropogenic species like  $\text{CO}$ ,  $\text{NO}_x$ , and NMHC. According to model calculations with a 2-D tropospheric model by Isaksen and Hov (1987), these species may have a significant impact on the production of tropospheric ozone, particularly at high northern latitudes, and can yield ozone increases of approximately 1 percent per year.

Changes in the chemical composition of the troposphere may also influence stratospheric ozone indirectly through changes in the oxidation rate of trace species such as  $\text{CH}_4$ ,  $\text{CH}_3\text{CCl}_3$ ,  $\text{CHF}_2\text{Cl}$ ,  $\text{CH}_3\text{Cl}$ , and  $\text{CH}_3\text{Br}$ . The atmospheric lifetimes of these species, and hence their concentrations, are determined by the tropospheric distribution of the hydroxyl radical,  $\text{OH}$ . It has long been known in tropospheric modelling that increases in  $\text{CH}_4$  and  $\text{CO}$  can markedly reduce global  $\text{OH}$  (Sze, 1977) and that this may have occurred over the past few decades (Thompson and Cicerone, 1986). Increases in the  $\text{NO}_x$  levels, on the other hand, will increase  $\text{OH}$  levels through a more efficient conversion of  $\text{HO}_2$  to  $\text{OH}$  through reaction with  $\text{NO}$ . In model calculations, Isaksen and Hov (1987) showed that the 1 percent per year growth in  $\text{CH}_4$  coupled with a 3 percent per year growth in anthropogenic releases of  $\text{CO}$ , NMHC, and  $\text{NO}_x$  would produce little net change in tropospheric  $\text{OH}$ . Modelling of tropospheric chemistry is inherently more complex because of the greater range of heterogeneity in the troposphere; tropospheric results from the current 2-D stratospheric models must be regarded with caution.

## THEORY AND OBSERVATIONS

### 7.3.6 Future Ozone Changes (1985–1990)

For the 7 years 1979–1985, trace gases and the solar cycle are calculated to act on ozone in the same direction. However, after 1985, trace gases and the solar cycle are expected to act on ozone in opposite directions as the increasing solar UV (ozone increases) is counteracted by the increase in stratospheric chlorine (ozone decreases). Figure 7.17 shows the calculated changes in globally averaged column ozone over one cycle from solar maximum to solar maximum, 1979–1990. Results from the Oslo model are shown for both the large and small solar-cycle cases. In the large solar-cycle case, the ozone changes from 1985 to 1990 are still dominated by solar-cycle effects, and ozone is predicted to increase by approximately 1.5 percent. In the small solar-cycle case, trace-gas effects are comparable, and total ozone increases are small, of the order 0.3 percent, from 1985 to 1990.

The picture is quite different when we look at predicted column ozone changes as a function of latitude where the trace gases have distinct fingerprints (i.e., largest depletions at high latitudes) and where the solar-cycle effects are uniform. Ozone increases from 1985 to 1990 in the large solar-cycle case are substantially smaller at high latitudes than for the global average. In the small solar-cycle case, trace gases dominate over solar cycle effects at mid- and high latitudes, leading to ozone decreases.

Over the next 5 years, detection and clear identification of the trace-gas signal in stratospheric ozone will require an accurate model for the solar cycle and its impact on ozone. Ozone trends in the near future depend critically on the magnitude of the solar UV variations. It is important to remember that, after 1991, when the solar cycle and trace gases again act in the same sense, total ozone is expected to decrease.

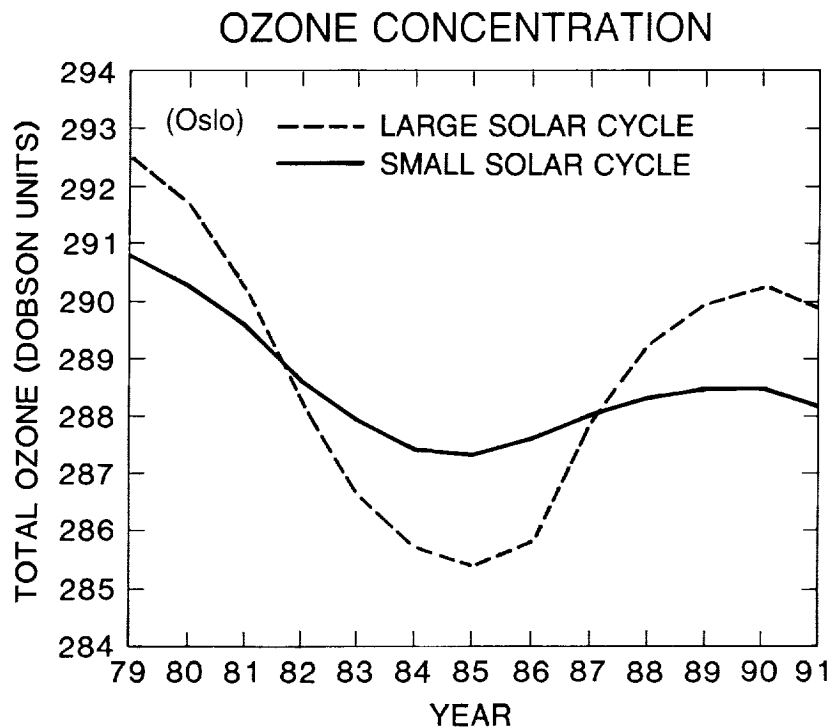


**Figure 7.17** Model calculations (Oslo) of globally averaged column ozone (Dobson Units) from 1979 extended to 1991 for the large (dashed line) and small (solid line) solar-cycle variations.

### 7.3.7 How Good Are the Models?

The models participating in this study have a certain degree of realism in that they can predict absolute concentrations of ozone, including its latitudinal, altitudinal, and seasonal variations. This general success of the models regarding ozone does not, of course, imply that the models can correctly describe all the remaining chemical species of the stratosphere. Nor, for that matter, does it imply that perturbations to ozone can be predicted with great confidence.

In this study we have made several systematic comparisons among the four 2-D models. These intercomparisons show a good qualitative, and even quantitative, agreement between the models in most cases. Some of the disagreement can be understood from the differences in model structure. However, there are important differences in predictions for the lower stratosphere, which clearly underline the need for further comparisons both among models and between models and observations, especially in the lower stratosphere. The ultimate test of predicting trends with these models would be a comparison between calculated and observed variations on a time scale of decades, such as we have attempted here with only limited global data.

An obvious failing of all the stratospheric models used in assessing future perturbations to ozone was the Antarctic ozone hole. From intensive studies of the Antarctic ozone problem (see Chapter 11) we have found that PSC's play a major role in the gas-phase chemistry of the lower stratosphere, and even have identified an important new species in the laboratory,  $\text{Cl}_2\text{O}_2$ , with a new catalytic cycle for destruction of ozone. Furthermore, we have recognized the unique stratospheric circulation associated with the Southern Hemisphere, in particular the isolation of the springtime Antarctic vortex. We have found unusually low levels of long-lived trace gases ( $\text{N}_2\text{O}$ , CFC's) in the wintertime lower stratosphere over both poles. These recent findings have led to substantial revisions both to the chemistry and transport of stratospheric models, but the changes to the models will not fix all of the discrepancies with regard to observations. Most of these improvements have not yet been applied to the type of calculations described here, although in the next 2 years we should expect to see assessments of future ozone change, including the effects of heterogeneous chemistry, PSC's and precipitation, and winter polar vortices.

Future studies and assessments should attempt to improve our confidence in the stratospheric models by addressing the following questions:

- Which species should we measure to provide key tests of models?
- Can we design strategies to detect early changes in the ozone?
- How do we define a "good fit" between models and observations?

## 7.4 CONCLUSIONS

Ozone concentrations in the atmosphere vary on different time scales and for several different causes. The models described in this chapter are designed to simulate the effect on ozone of changes in the concentration of such trace gases as CFC,  $\text{CH}_4$ ,  $\text{N}_2\text{O}$ , and  $\text{CO}_2$ . Changes from year to year in UV radiation associated with the solar cycle are also included in the models. A third source of variability explicitly considered is the sporadic introduction of large amounts of  $\text{NO}_x$  into the stratosphere during atmospheric nuclear tests.

## THEORY AND OBSERVATIONS

On the other hand, the models are not designed to simulate variations associated with weekly meteorological variations, but should be able to calculate the average seasonal variation. Thus, the effects of the pronounced QBO in the wind systems of the lower stratosphere and of the ENSO on circulation of the tropical troposphere are not considered in the models. Another important limitation of the models is that they do not attempt to simulate effects of volcanic eruptions or of condensed-phase processes in general (i.e., heterogeneous chemistry and physics). This means that the Antarctic ozone hole does not show up in any of the model simulations discussed here.

The performance of the models has been tested by comparing the simulations against observations of ozone and some other key chemical compounds. The observations exhibit substantial variability in both space and time that is not reflected in the model simulation. Nevertheless the average seasonal variations of the ozone concentration as a function of height and latitude are simulated quite well. We have difficulty quantifying the uncertainty associated with the calculations of ozone changes due to systematic changes in forcing, such as increasing concentrations of CFC's. The ultimate test of the models in this context is a comparison between calculated and observed variations on time scales of years to decades.

A major source of uncertainty in 2-D models is the treatment of the troposphere: its chemistry, its zonal inhomogeneities, and the ability to predict changes in tropospheric ozone due to trace gas changes ( $\text{CH}_4$ ,  $\text{NO}_x$ , NMHC's, CO). Over the time period considered here, increases in tropospheric  $\text{CH}_4$ , CO, and  $\text{NO}_x$  are likely to have led to significant increases in tropospheric ozone. Changes in tropospheric ozone may be large enough (~10 percent) to obscure small changes (~1 percent) in total column ozone resulting from changes in the stratosphere.

The series of atmospheric nuclear tests during the late 1950's to early 1960's represent an interesting test case. All four models show a substantial, though different, depletion of total ozone during the year following the large explosion in late 1962. A depletion of similar magnitude seems to be borne out by the observations of total ozone. However, the data are sparse and may not be representative of this period. Furthermore, the observed decrease in ozone appeared to start prior to the main bomb tests. No firm conclusions can be drawn from this simulation of the atmospheric nuclear tests.

Calculated changes in ozone due to increasing trace gas have specific patterns with latitude, altitude, and season (i.e., fingerprints) that differ from those resulting from solar-cycle variations. The primary impact of the trace-gas scenario is due to increasing levels of stratospheric chlorine. The fingerprint on column ozone of the trace gases for 1979–1985 shows a maximum variation at high latitude, with larger decreases occurring during late winter (0.75–1.5) percent and smaller decreases during summer (0.25–0.5) percent. A uniform decrease of 0.3–0.5 percent over the Tropics is estimated in the three models for which comparisons are available. The corresponding vertical profiles show depletion peaked at 40 km of the order of 7–10 percent at high latitudes and 3–5 percent in the Tropics.

As solar activity declines from maximum to minimum (1979 to 1985), the column ozone is predicted to decrease almost uniformly across all latitudes and seasons. The magnitude of this change in column ozone depends on the UV variations and ranges from about -2 percent for the large solar-cycle case to about -0.7 percent for the small solar-cycle case. The corresponding profiles decrease everywhere above 25 km with a broad extreme of about -3 percent near 40 km—a pattern that is less pronounced but similar to that from increases in CFC's.

Can we distinguish between solar-cycle changes in ozone and those induced by increases in CFC's and CH<sub>4</sub>? The answer to this question requires the testing of all aspects of the fingerprints of the two perturbing influences. The first approach is to look at the long-term record from the Dobson network in a search for a cyclic change in column ozone that is correlated with solar activity over the solar cycle. The statistical uncertainty of the observed amplitude is large, and the solar cycle amplitude not well known. For this reason, the trace-gas signal cannot be clearly separated from the record by subtracting the solar effect.

Another approach used to remove the effects of the solar cycle and short-term variations is to average the Dobson record over two separate 11-year periods, assuming that different solar cycles have the same integrated impact on column ozone. Wintertime Dobson data for 1976–1986 are consistently lower than those from 1965–1975. The change was most pronounced at high- and midlatitudes (50–60°N), and about -3 percent at 60°N. This observed decrease in ozone over the period is substantially larger than that predicted by 2-D models on the basis of the adopted trace gas scenarios. The pattern is similar to the trace-gas fingerprint, indicating the possibility that the trace-gas effect is underpredicted. This is not sufficient reason, however, merely to scale the results for the trace-gas scenario without determining the source of error, such as the omission of certain physics and chemistry from the models.

The satellite data from TOMS/SBUV provide a more global picture of ozone, but only since late 1978. This period, 1979–1986, is one in which both the solar cycle and trace gases are expected to act in the same sense—that is, to reduce column ozone. The pattern of changes observed by TOMS corroborates the evidence from the 11-year average of the Dobson data: large decreases in ozone have occurred at high latitudes in both hemispheres in winter. To obtain a separation of the fingerprints of trace gases and solar cycle, global satellite data *must* be extended through the next solar maximum (circa 1991).

The observed changes in ozone concentration at different altitudes may also provide evidence of specific perturbations. The most reliable record for absolute changes in ozone profiles over the past decade is limited to satellite instruments, SAGE-I and SAGE-II, and to the recently analyzed Umkehr data (see Chapter 5). The difference between average ozone profiles from the SAGE instruments in 1979 and 1985 show a maximum change near 40 km of  $-4 \pm 4$  percent, and from the Umkehr observations  $-9 \pm 5$  percent between 1979 and 1986. This should be compared with a range of -6 percent to -10 percent predicted for the combined effects of increase in CFC's and decrease in solar UV. Although the decrease appears to be dominated by trace gases, the height profile is not sufficiently unique to make a definitive identification of fingerprints from trace gases.

The effect of the solar cycle on ozone after its passing through its minimum during 1985 is expected to be opposite that of the trace gases until the next solar maximum. Knowledge of the magnitude of the solar cycle impact is essential for predicting the change in total ozone during this period. The large solar-cycle case gives ozone changes that dominate over trace gas effects at all latitudes through 1990. Calculations using this model for solar variability predict an increase in globally averaged column ozone greater than 1 percent over this period. However, the small solar-cycle model with a less pronounced solar variation in UV flux gives ozone changes that are near zero over the next few years. Furthermore, the small solar-cycle model gives a distinct fingerprint over the next few years in which total ozone increases at low latitudes (solar-cycle effects dominate) and decreases at high latitudes (trace-gas effects dominate).

## THEORY AND OBSERVATIONS

Obviously, our lack of knowledge of the magnitude of the solar-cycle variations in the UV limits our ability to identify fingerprints in the observed ozone changes over the next few years. Furthermore, the prediction of future ozone depletion from trace gases with the current 2-D models is uncertain because of the lack of heterogeneous chemistry in the models used here. We are still unsure whether the discrepancy between models and observations in the Northern Hemisphere over the past 20 years is statistically significant and, even if it is, we are unable to say how this error will propagate for future predictions of ozone.